

## Article

# Comparison of the Techno-Economic and Environmental Assessment of Hydrodynamic Cavitation and Mechanical Stirring Reactors for the Production of Sustainable *Hevea brasiliensis* Ethyl Ester

Olusegun David Samuel <sup>1,2</sup>, Peter A. Aigba <sup>1</sup>, Thien Khanh Tran <sup>3,4,\*</sup>, H. Fayaz <sup>5</sup>, Carlo Pastore <sup>6</sup>,  
Oguzhan Der <sup>7</sup>, Ali Erçetin <sup>8</sup>, Christopher C. Enweremadu <sup>2</sup> and Ahmad Mustafa <sup>9,10</sup>

- <sup>1</sup> Department of Mechanical Engineering, Federal University of Petroleum Resources, P.M.B 1221, Effurun 330102, Delta State, Nigeria; samuel.david@fupre.edu.ng (O.D.S.); paaigba@yahoo.com (P.A.A.)
  - <sup>2</sup> Department of Mechanical Engineering, University of South Africa, Science Campus, Private Bag X6, Florida 1709, South Africa; enwercc@unisa.ac.za
  - <sup>3</sup> Advanced Applied Sciences Research Group, Dong Nai Technology University, Bien Hoa City 76100, Vietnam
  - <sup>4</sup> Faculty of Technology, Dong Nai Technology University, Bien Hoa City 76100, Vietnam
  - <sup>5</sup> Power Generation Unit, Institute of Power Engineering (IPE), Universiti Tenaga Nasional, Kajang 43000, Malaysia; katperfayaz@ieee.org
  - <sup>6</sup> Water Research Institute (IRSA), National Research Council (CNR), via F. de Blasio 5, 70132 Bari, Italy; carlo.pastore@ba.irs.cnr.it
  - <sup>7</sup> Department of Maritime Vehicles Management Engineering, Maritime Faculty, Bandırma Onyedi Eylül University, 10200 Bandırma, Turkey; oder@bandirma.edu.tr
  - <sup>8</sup> Department of Naval Architecture and Marine Engineering, Maritime Faculty, Bandırma Onyedi Eylül University, 10200 Bandırma, Turkey; aercetin@bandirma.edu.tr
  - <sup>9</sup> Faculty of Engineering, October University for Modern Sciences and Arts (MSA), Giza 12451, Egypt; ammhamed@msa.edu.eg
  - <sup>10</sup> Center of Excellence, October University for Modern Sciences and Arts (MSA), Giza 12451, Egypt
- \* Correspondence: tranthienkhanh@dnpu.edu.vn



**Citation:** Samuel, O.D.; Aigba, P.A.; Tran, T.K.; Fayaz, H.; Pastore, C.; Der, O.; Erçetin, A.; Enweremadu, C.C.; Mustafa, A. Comparison of the Techno-Economic and Environmental Assessment of Hydrodynamic Cavitation and Mechanical Stirring Reactors for the Production of Sustainable *Hevea brasiliensis* Ethyl Ester. *Sustainability* **2023**, *15*, 16287. <https://doi.org/10.3390/su152316287>

Academic Editors: Domenico Licursi and Juan Hernández Adrover

Received: 8 October 2023

Revised: 19 November 2023

Accepted: 20 November 2023

Published: 24 November 2023



**Copyright:** © 2023 by the authors. Licensee MDPI, Basel, Switzerland. This article is an open access article distributed under the terms and conditions of the Creative Commons Attribution (CC BY) license (<https://creativecommons.org/licenses/by/4.0/>).

**Abstract:** Even though the hydrodynamic cavitation reactor (HCR) performs better than the mechanical stirring reactor (MSR) at producing biodiesel, and the ethylic process of biodiesel production is entirely bio-based and environmentally friendly, non-homogeneous ethanol with the triglyceride of underutilized oil, despite the many technical advantages, has discouraged the biodiesel industry and stakeholders from producing ethylic biodiesel in HCRs. This study examines the generation of biodiesel from rubber seed oil (RSO) by comparing the ethyl-based HCR and MSR. Despite ethyl's technical advantages and environmental friendliness, a lack of scalable protocols for various feedstocks hinders its global adoption. The research employs Aspen HYSYS simulations to investigate the ethanolysis process for RSO in both HCRs and MSRs. The HCR proves more productive, converting 99.01% of RSO compared to the MSR's 94.85%. The HCR's exergetic efficiency is 89.56% vs. the MSR's 54.92%, with significantly lower energy usage. Removing catalytic and glycerin purification stages impacts both processes, with HC showing lower exergy destruction. Economic analysis reveals the HCR's lower investment cost and higher net present value (USD 57.2 million) and return on investment (176%) compared to the MSR's. The HCR also has a much smaller carbon footprint, emitting 7.2 t CO<sub>2</sub> eq./year, while the MSR emits 172 t CO<sub>2</sub> eq./year. This study provides database information for quickly scaling up the production of ethanolic biodiesel from non-edible and third-generation feedstocks in the HCR and MSR.

**Keywords:** biodiesel; exergy; transesterification; Aspen HYSYS; reactor technology; ethyl ester; sustainability; mechanical stirring; hydrodynamic cavitation; techno-economics

## 1. Introduction

Increasing the production and use of biofuels, such as biodiesel, in the transportation industry is now thought to be a workable way to cut back on the use of fossil fuels and the pollution that they cause. The deployment of biofuels as a sustainable substitute for fossil fuels has gained greater recognition during the last few decades. Biodiesel (BD), one of the most renowned biofuels, has tremendous potential to replace the scarce and non-renewable resources of fossil fuels [1]. Research on biodiesel is being driven by worldwide policies that fit with the implementation of Sustainable Development Goal 7 (SDG 7) [2]. These policies highlight the mitigation of climate change, renewable energy, and environmental sustainability as priorities. Improving farming practices, advocating for clean energy, and reducing carbon emissions are the main goals. Biodiesel technology research and development are being actively supported by international agreements and efforts. Sustainable production practices, waste reduction, and the utilization of a variety of feedstocks are all emphasized by these initiatives. Important international accords, such as the United Nations Framework Convention on Climate Change (UNFCCC) Paris Agreement, in conjunction with regional partnerships, are actively promoting sustainable energy alternatives [3]. Under SDG 2030, regulations encouraging biodiesel research are being implemented more quickly due to the urgent need to mitigate climate change.

The demand for BD adoption and its use in diesel engines could stem from its reduced emission profiles, non-toxicity, carbon neutrality, and renewability [1]. Despite these benefits, biodiesel's higher charge than diesel fuel has persisted. A higher percentage of biodiesel production costs emanate from edible oils [4]. Hence, the deployment of inedible and non-competitive generational oils (NCGOs) for BD production has been extensively investigated [5]. Yang et al. [6] hinted that the most common inedible and NCGO oily feedstock are jatropha, jojoba, mahua, moringa, Tung oil, camelina, castor oil, croton oil, milk bush, algae, neem, tobacco, RSO, etc. RSO is a preferred choice for BD over the other stated oils due to its similar oil qualities to regular diesel. Commercial BDs are synthesized using methylic and ethylic methods (ME and ER, respectively), as reported by Samuel et al. [7] and Yusuff et al. [8]. Samuel et al. [9] and Altamirano et al. [10] stated that ER will surpass ME due to its eco-friendliness, reduced emission profiles, and renewability. Mandari and Devarai [11] attributed the immiscibility of inedible and NCGOs during ER to a notable transesterification and a reduction in mass transfer rate. To enhance mass transfer and increase the contact surface area between reactants during BD manufacturing, MSR has been used on an industrial scale [12,13]. However, the MSR cannot adequately mix, and long reaction times, high energy consumption, excess molar ratios, and excessive catalyst doses constrain its effectiveness [14]. Most industrial biodiesel facilities use conventional batch reactors, but they have significant capital, operating, and reaction time costs and unneeded operational and production expenses [15,16].

Various technologies are employed in the production of biodiesel. Conventional reactors require longer reaction times, and using an extra-large reactor adds unnecessary costs to production and operation [16]. Several technologies have been developed to address the difficulty outlined above. The most prevalent types are hydrodynamic, acoustic, optical, and particle cavitation [17]. HCRs have recently emerged as a promising, extremely inventive technique for steadying the production of biodiesel [18]. The peculiar superiority of the HCR is due to its capacity to be better set up and effective in mixing non-miscible fluids compared to prolonged, unadventurous mechanical procedures [7]. The technique, known as hydro cavitation, occurs when a fluid passes through an opening and a pressure drop causes cavities to form appropriately. This method yields higher yields and shorter reaction times. The most cutting-edge technology for creating a cleaner biodiesel synthesis process is expected to be the HCR, ensuring a cleaner fuel production. Regarding conversion, alcohol-to-oil molar ratios, catalyst dose, reaction duration, and oily feedstock consumption, Maddikeri et al. [19], Chuah et al. [20], and Laosuttiwong et al. [21] proposed that HCRs might be more effective than MSRs. However, the techno-economic feasibility and environmental impact of HCR technology are not well understood by biofuel and

processing factories that employ it to produce ethyl ester biodiesel. The long-term success of biodiesel depends heavily on these variables.

Recent studies on the production of methyl biodiesel from feedstock in most developing nations utilizing HCRs and MSRs indicate that the technology has a promising future [22]. This result is consistent with previous studies on the production of biodiesel from RSO. A review of the literature indicates that the earlier studies on this area of study did not include basic process engineering studies, such as process simulation, scale-up studies, process design, and techno-economic studies of HCR and MSR-based ethylic biodiesel, which can increase the viability of RSO biodiesel production and commercialization. The technical and financial performance of a chemical process or product design can be assessed using the techno-economic analysis (TEA) technique. Process simulation and economic models use TEA to assess the feasibility and sustainability of new or emerging technologies [23]. It also considers a technology's worldwide cost–profit value, which helps prospective investors to make important financial decisions [24]. TEAs are useful not only for evaluating the overall economic viability before deployment but also for scaling up small-scale BD facilities.

The techno-economic elements of producing biodiesel from different oils have been analyzed and upgraded through the use of commercial process simulators such as Aspen Plus<sup>®</sup>, HYSYS<sup>®</sup>, and Superpro [24,25]. By incorporating these simulators with the Aspen capital cost estimator, researchers and stakeholders may define material, mass, and energy balances and build an extensive cost database. HCRs are preferred over conventional reactors and other intensification techniques, including tube, microwave, ultrasonic, spinning disk, and supercritical conditions. HCRs are desired due to their superior mixing capabilities, reduced reaction duration, and ability to enhance fuel properties [7]. The TEA of biodiesels from oily feedstocks, particularly in HCRs, has a research gap that is highlighted in Appendix Table A1. The TEA of methylic BD catalyzed by lipase and a sonicator has received less attention than methylic-based HCRs in previous investigations. Notably, there is a lack of TEA studies on second-generation oily feedstocks like rubber seed oil and ethanol for transesterification. Furthermore, no study has been conducted on the TEA, environmental assessment, or comparison with conventional reactors of ethylic BD produced by an HCR. To assure 100% bio-based scaling up and economically viable biofuel industries, the following measures were implemented in response to the lack of such studies in the literature: (i) modelling a cavitation system and a cleaner rubber seed oil ethyl ester based on a conventional reactor, (ii) developing an in-depth technical, financial, and environmental analysis contrasting the well-established MSR, and (iii) comparing the long-established MSR [13] with the suggested HCR [26] in depth on technological, financial, and environmental fronts.

## 2. Materials and Methods

### *Process Description and Assumption*

The present study utilized simulation models to conduct a detailed comparative analysis of the biodiesel synthesis processes of MSRs and HCRs. The simulation process generated a large amount of design data, including mass balance and energy, in addition to other thermodynamic operating data. The transesterification reaction between RSO and ethanol was carried out with potassium hydroxide acting as a catalyst. RSO is represented by triolein while the biodiesel product is represented by ethyl oleate (C<sub>19</sub>H<sub>36</sub>O<sub>2</sub>). The downstream processes comprises catalyst neutralization and unreacted ethanol removal (only for MS process). As glycerin and biodiesel are hydrophilic and hydrophobic, water washing was used as a separation technique. After applying phosphoric acid to the acquired potassium hydroxide phase to neutralize its pH, the sodium phosphate that was left behind was isolated. The principal reaction outputs were thought to be glycerin and biodiesel. Vacuum distillation was used to remove the unreacted ethanol (only in MS-based processes) and return it to the mixture along with fresh ethanol as fuel.

Conversely, the HC process scenario is a case study inquiry that employs HCR, utilizing the same quantitative features and process parameters as the MS process. For the first time, the HC system was modelled in this study as a pump, throttling valve, and plug flow reactor (PFR) [26]. The hydrodynamic cavitation phenomenon is caused by mechanical constriction brought on by a throttling valve (VLV-100) that creates a pressure differential large enough to result in the creation of vapour bubbles or cavities. High energy is released when the pressure drops from 4 bar to 0.2 bar below the reaction mixture's vapour pressure (0.3 bar). This causes vapour cavities to collapse. By overcoming the immiscibility of the oil and ethanol phases and improving the physical and chemical transformation mixture, this energy increases mass transfer, which in turn increases reaction rate and decreases residence time. With the exception of the tower requirement, the remaining steps of the process are essentially similar to those of the MS process. Figure 1 depicts the entire reaction process.

The following are the assumptions on the thermodynamic characteristics of ethyl ester biodiesel:

- The atmospheric temperature and pressure are fixed at 25 °C and 1 bar, respectively.
- Pressure drops in pipelines and heat exchangers are disregarded.
- The RSO is modelled using triolein, with an assumed conversion rate of 95% [27].
- Every process is assumed to be in a steady-state, adiabatic condition.
- Any changes to the fluid's kinetic and potential energy are regarded as negligible.
- Pumps and compressors are supposed to have an adiabatic efficiency of 85%, the distillation tray tower to have an efficiency of 65%, and the electrical generator (motor) to have an efficiency of 96%.
- The transesterification process operates continuously in a steady-state mode.
- The MS process consists of a transesterification unit, glycerine purification unit, and biodiesel distillation unit. The glycerine purification unit involves washing the biodiesel with water to remove glycerine, potassium hydroxide removal through phosphoric acid addition, and the subsequent removal of potassium phosphate.
- A glycerine purification unit and a transesterification unit make up the HC process.
- Ethanol recovery is considered only in the MS process, while it is disregarded in the HC process due to the high conversion rate of over 99%.

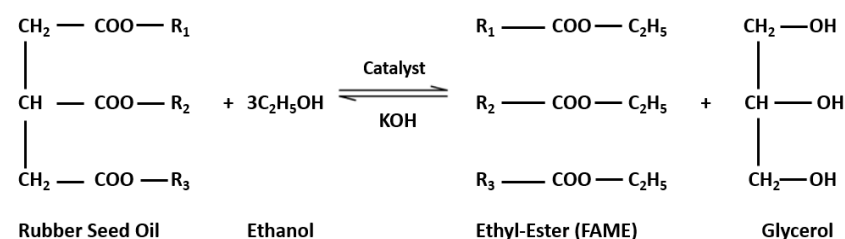


Figure 1. Transesterification reaction process [28].

### 3. Modelling and Analysis

Aspen HYSYS, v10, which is widely recognized for its broad applicability in biofuels and other similar emerging feedstock research, was used to model the transesterification processes for biodiesel generation using the MSR and HCR techniques [29]. This simulation was approached through certain fundamental steps such as transesterification, washing with water or neutralization or catalytic removal, ethanol recovery, and biodiesel purification. A nonrandom two-liquid (NRTL) model was employed in Aspen HYSYS as the thermodynamic fluid package since the reactants, ethanol and glycerol, are polar substances. The alcohol-to-oil molar ratio is adjusted to 3:1 [30]. In order to prevent the production of ethanol vapour, RSO is injected into the preheated continuously stirred tank reactor (CSTR) at a temperature of 60 °C and a pressure of 4 bar as triolein (feedstock) in the MS process.

The conversion reactor, represented by the CSTR in this model, is necessary for handling thermodynamic and kinetic data, including the activation energy ( $E$ ) and Arrhenius constant ( $A$ ), which are produced by RSO during research. RSO ethyl esters (biodiesel) and glycerol are produced at this stage when the RSO reacts with ethanol in the presence of a homogeneous catalyst, specifically KOH. This stream enters a separation column (Splitter-1) where the content is cleaned with water to help to separate the alcohol and ethyl oleate mixture at the top of the separator into a distillation tower, where the salt is processed into the catalytic reactor at the bottom and the ethanol is recycled back into the process to produce biodiesel. However, the salt is further processed in a catalytic reaction vessel (Cata-RXR) where  $H_3PO_4$  is encountered to neutralize the content and release water vapour at the top and transfer the recovered mixture from the bottom into the Splitter-2 separator, where glycerol and  $K_3PO_4$  are recovered at the top and bottom, respectively. Figure 2 depicts the distinct process streams.

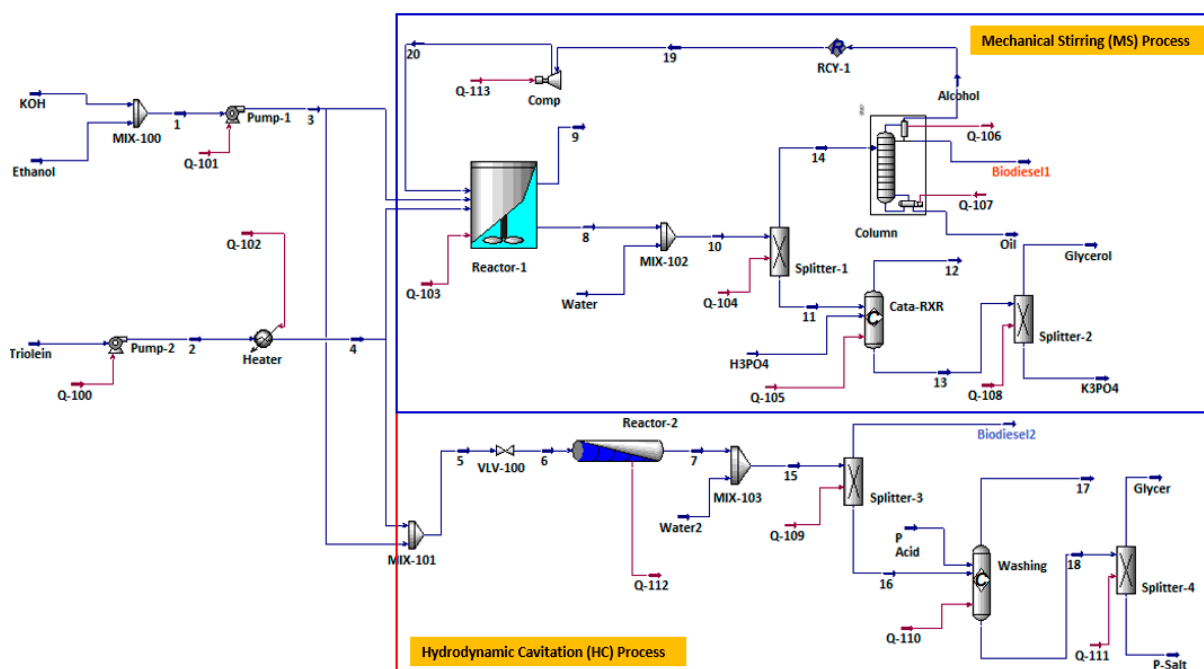


Figure 2. Combined MS and HC same-source processes feed streams.

### 3.1. Energy Analysis

The Arrhenius equation predicts that a small increase in reaction temperature will result in a significant increase in the reaction rate constant magnitude,  $k$ , defined by Equation (1). This prediction is based on the kinetic data of the transesterification reaction obtained from the literature [31].

$$k = A * \exp\left(\frac{-E_a}{RT}\right) \quad (1)$$

where  $A$  is the pre-exponential factor,  $E_a$  is the activation energy,  $R$  is the ideal gas constant 8.314 (J/Kmol), and  $T$  is the absolute temperature. The reaction rate constant and the activation energy are considered as  $0.063 \text{ min}^{-1}$  and 29,800 kJ/kg. mol, respectively [31]. As discussed, when a pressure differential is established across the upstream valve, which is utilized to enhance the cavitation phenomena in the HC process, care must be taken to prevent any jet erosion occurrence. Equation (2) is utilized to determine the cavitation

number,  $\sigma$ , which is crucial for forecasting cavitation and its possible impacts, or its effectiveness, in the HC reaction process [32,33] from Equation (2)

$$\sigma = \frac{P_f - P_v}{\frac{1}{2}\rho V^2} \quad (2)$$

where  $P_f$  and  $P_v$  (pa) are the outlet and vapour pressure of the reaction mixture, the density of the reaction mixture is  $\rho$ , ( $\text{kg}/\text{m}^3$ ), and  $V$  ( $\text{m}/\text{s}$ ) is the flow velocity through the constriction section, which can be evaluated by knowing the upstream flow rate and diameter of the constriction hole. A higher conversion yield is produced when the cavitation number is decreased because the reactive mixture stays in the cavitation zone for a longer period of time. With the exception of preheating the feed before introducing it to the HCR, the energy created is added to the reaction mixture. This highlights the HC process's intriguing potential for energy savings over the MS process. Furthermore, Equation (3) can be used to evaluate the energy released,  $E$ , in the HC reactor [34].

$$\dot{E} = Q_F * \Delta P \quad (3)$$

where  $Q_F$  is the volumetric flow of the liquid reaction mixture ( $\text{m}^3/\text{s}$ ) and  $\Delta P$  is the pressure change (kpa) through the constriction.

### 3.2. Exergy Analysis

The mass, energy, and energy balance general expressions of the rubber seed oil biodiesel plant at a control volume (CV) are estimated in this section. In other words, mass balance (continuity) is expressed by Equation (4), and any energy changes over the boundary are considered to be negligible.

$$\sum \dot{m}_{in} = \sum \dot{m}_{Out} \quad (4)$$

To evaluate the energy balance of the streams, Aspen Plus was used. Energy is induced in the system by the mass flow rate, work output, and energy released into the surrounding environment. Equations (5)–(7) can therefore be utilized to give energy balance in control volume at the steady state.

Equation (8) expresses the entropy balance produced by the same process, while Equation (7) is obtained by applying the first law of thermodynamics at a control volume (CV).

$$\dot{E}_{in} - \dot{E}_{Out} = \frac{dE_{system}}{dt} = 0 \implies \text{steady} \quad (5)$$

$$\sum \dot{E}_{in} = \sum \dot{E}_{Out} \quad (6)$$

$$\sum Q - \sum \dot{W} = \sum \dot{E}_{Out} - \sum \dot{E}_{in} \quad (7)$$

$$\sum \dot{m}_{in} s_{in} + \sum \frac{Q_{CV}}{T} + \dot{S}_{gen} = \sum \dot{m}_{Out} s_{Out} \quad (8)$$

Energy losses, energy destruction, component improvement potentials, and energy efficiencies are the main ideas examined from an exergy fundamental point of view. Equation (9) is used to compute the exergy balance for each component under steady-state conditions [35].

Equation (9), in contrast to energy, states that exergy is not irreversibly destructible within a control container. In order to create a thermodynamic process flowsheet that will aid in the various destroyed exergy calculations of the system's components, the biodiesel synthesis process is simulated in this work. To define exergy destruction, Equation (9) is modified as shown in Equation (10).

Equations (12) and (13) describe, respectively, the exergetic work performed and the heat flow across the control volume of each component.

Equation (14) can be employed for expressing flow exergy. Equation (14) transforms into Equation (15) due to the negligible kinetic and potential components of flow exergy. Additionally, Equation (16) represents the physical exergy component of flow exergy.

$$Ex_{in} - Ex_{Out} - Ex_D = \frac{dE_{system}}{dt} = 0 \implies steady \quad (9)$$

$$Ex_D = Ex_{in} - Ex_{Out} \quad (10)$$

Or, more broadly, as

$$Ex_D = \sum \dot{m}_{in} ex_{in} + \sum Ex_{Q, in} + \sum Ex_{W, in} - (\sum \dot{m}_{out} ex_{out} + \sum Ex_{Q, out} + \sum Ex_{W, out}) \quad (11)$$

where  $\dot{m}$ ,  $\dot{E}$ ,  $Ex$ ,  $Ex_W$ , and  $Ex_Q$  represent the inlet and outlet flow of mass, energy, exergy, work, and power transfer rates, respectively.

$$Ex_W = W \quad (12)$$

$$Ex_Q = \left(1 - \frac{T_o}{T}\right) Q \quad (13)$$

$$e_x = Ex_{KE} + Ex_{PE} + Ex_{CHM} + Ex_{PHY} \quad (14)$$

$$ex_{flow} = ex_{CHM} + ex_{PHY} \quad (15)$$

$$ex_{PHY} = (h - h_o) - T_o(s - s_o) \quad (16)$$

$$Ex_{CHM} = \sum_i y_i \bar{ex}_i^{CHM} + \bar{R}T_o \sum_i y_i \ln(y_i) \quad (17)$$

where  $y_i$  is the component  $i$  molar fraction in the gaseous mixture gas,  $\bar{ex}_i^{CHM}$  is the standard exergy of the constituent,  $h$  and  $s$  are the enthalpy and entropy generated, and  $R$  is the universal gas constant.

Equations (18) and (19) present the ratio of the chemical exergy of fuel to the LHV. The chemical exergy of fuel can also be expressed in terms of the LHV of solid or liquid fuel [36,37].

The chemical exergy of a stream is computed using Equation (20), and it can also be computed as flow, as illustrated in Equation (21).

Equation (22) calculates the ratio of energy intake to energy destruction in a component, which is known as energy fuel depletion. Additionally, the rate of irreversibility is shown as a ratio in Equation (23). Equation (24), however, defines the components' potential for improvement.

The system's overall exergy efficiency and its component exergy efficiencies can be determined using Equations (25) and (26).

For operational component assessment, Tsatsaronis and Lazzaretto [38] proposed and established a fuel and product exergy model. As shown in Table 1, the transesterification and neutralization processes were assessed in this study using the strategy by Boyano et al. [39].

$$\varphi = \frac{ex_F^{CH}}{LHV} \quad (18)$$

$$\varphi = 1.0401 + 0.1728\left(\frac{h}{c}\right) + 0.0432\left(\frac{o}{c}\right) + 0.2169\left(\frac{s}{c}\right) * \left(1 - 2.0628\frac{h}{c}\right) \quad (19)$$

where  $c$ ,  $h$ ,  $s$ ,  $o$ , and  $\varphi$  are the mass fractions of carbon, hydrogen, sulfur, and oxygen, respectively [37, 40,41].

$$Ex_{CHM} = \dot{m}_i ex^{CHM} \quad (20)$$

$$Ex_{flow}^{CH} = \Delta G_f + \sum_i ex_i N_i \quad (21)$$

where  $\Delta G_f$  is the standard Gibbs free energy of the formation of the reactants,  $ex_i$  is the  $i$ th pure elemental component chemical exergy of the substance, and  $N_i$  is the  $i$ th pure elemental molar fraction of the substance.

**Table 1.** Biodiesel process exergy balance equations.

Processes	Techniques	Exergy Balance Equation
Transesterification	MS	$Ex_D = (Ex_3 + Ex_4 + Ex_{20} + Ex_Q) - Ex_8 + Ex_9$
	HC	$Ex_D = Ex_6 - (Ex_{Q-112P} + Ex_7)$
Neutralization (catalyst removal)	MS	$Ex_D = (Ex_{11} + Ex_{H_3PO_4} + Ex_Q) - Ex_{12} + Ex_{13}$
	HC	$Ex_D = Ex_{16} + Ex_{PACID} + Ex_{Q-110P} - (Ex_{17} + Ex_{18})$
Ethanol recovery	MS	$Ex_D = (Ex_{14} - Ex_{19}) + Ex_{Q-107P} - ((Ex_{oil} - Ex_{14}) + Ex_{Q-106P} + Ex_{biodiel1})$
Glycerol purification	MS	$Ex_D = Ex_{13} + Ex_{Q-108P} - Ex_{K_3PO_4} + Ex_{GLYCEROL}$
	HC	$Ex_D = Ex_{18} + Ex_{Q-111P} - Ex_{PSALT} + Ex_{GLYCER}$
SPLITTER-1	MS	$Ex_D = Ex_{10} + Ex_{Q-104P} - Ex_{12} + Ex_{13}$
MIX-100	MS/HC	$Ex_D = (Ex_{KOH} + Ex_{ETHANOL}) - Ex_1$
MIX-102	MS	$Ex_D = (Ex_8 + Ex_{WATER}) - Ex_{10}$
PUMP-1	MS/HC	$Ex_D = Ex_1 + Ex_{Q-101P} - Ex_3$
COMPRESSOR	MS	$Ex_D = Ex_{19} + Ex_{Q-113P} - Ex_{20}$
VLV-100	HC	$Ex_D = Ex_5 - Ex_6$
MIX-101	HC	$Ex_D = (Ex_3 + Ex_4) - Ex_5$
MIX-103	HC	$Ex_D = (Ex_7 + Ex_{WATER-2}) - Ex_{15}$
HEATER	MS/HC	$Ex_D = (Ex_2 + Ex_{Q-102P}) - Ex_4$
PUMP-2	MC/HC	$Ex_D = Ex_{TRIOLEIN} + Ex_{Q-100P} - Ex_2$

Equations (22)–(24) provide the relative ratios of the component's exergetic destruction to its total exergy destruction and component improvement in the plant [35]. Equations (25) and (26) provide the energy and energy efficiency, respectively.

$$y_D = \frac{Ex_D}{Ex_{in,tot}} \quad (22)$$

$$y_{D,i}^* = \frac{Ex_{D,i}}{Ex_{D,tot}} \quad (23)$$

$$IP_i = \left(1 - \frac{\eta_{ex}}{100}\right) Ex_{D,i} \quad (24)$$

$$\text{Energy efficiency, } \eta_{\dot{E}} = \frac{\text{Energy Output}}{\text{Energy Input}} \quad (25)$$

$$\text{Exergy efficiency, } \psi_{Ex} = \frac{\text{product Exergy}}{\text{Fuel exergy}} = 1 - \frac{Ex_D}{\text{Fuel exergy}} \quad (26)$$

#### 4. Economic Model Analysis

In order to evaluate the project's viability, the sources of income, project expenses, and cash flow analysis are all determined using the economic models in this study. By providing a variable summary that may be utilized as a selection tool for the most suitable and economical (MS vs. HC) process for investment objectives, this techno-economic comparison study helps the biodiesel community. Due to a capacity factor of 90.4% for the biodiesel plant, the economic assessment projected 7920 operating hours annually.

##### 4.1. Summary of Total Capital Investment

The importance of accurately computing the total capital investment for this fictitious project by adding the necessary fixed capital investment, working capital, and initial expenditure is examined [42]. Therefore, it is crucial to consider the long-term total spending investment in light of how it affects the plant's planning [43]. The necessity of avoiding unrealistic budgets highlights the importance of precise costing, which includes engineering, inside and outside battery limits (ISBLs and OSBLs), and contingency expenses for various production-related accessories and equipment. To calculate the ISBL cost, a variety of estimating techniques can be applied, including those by Bridgewater, Taylor, Gore, Stallworthy, Klumpar, Brown, and Fromme [44]. Bridgewater's approach was used for the MS and HC plants. Accurate results from Bridgewater's methodologies depend on

knowing the reactor's conversion rate, plant capacity, and number of main units. For the HC and MS plants, the productivity of the plants and the conversion rates were found to be 224 and 207 tons, respectively, based on Aspen estimates. Lastly, Bridgewater's method was used to compute the ISBL cost via Equation (27).

The OSBL cost encompasses off-site developments for plant operation and normally ranges from 10% to 100% [24]. However, a 30% OSBL proportion was applied in this work. Since the company's research team already had the required package, engineering fees were not included. To offset unforeseen costs, a contingency sum of 10% was set out for MS technology and 15% for HC technology. A total of 15% of the direct capital cost was set aside as working capital [43]. To sum up, 10% of the combined costs of OSBL and ISBL were allocated to start-up costs. Table 2 presents other economic hypotheses used in the present study.

$$C = 280,000N \left( \frac{Q}{s} \right)^{0.3} \quad (27)$$

where C represents the ISBL capital cost (USD), N is the number of main units, Q is the plant capacity (t/year), and s is the reactor conversion rate.

$$\text{Total Project Cost} = \text{Direct Costs} + \text{Indirect Costs} \quad (28)$$

**Table 2.** Economic assumptions and evaluation parameters [24,43].

Economic Assumptions	Parameters
Cost of equity	25%
Cost of debt	5%
Cost of capital	15%
Debt ratio	0.5
Discount rate	11%
Tax rate	22.50%
Depreciation method	Straight-line
Depreciation period	10 years
Depreciation rate	10%
1st year direct fixed capital (DFC)	30%
2nd year direct fixed capital (DFC)	70%
Project life	15 years

#### 4.2. Operating Cost Expenses

Costs associated with both fixed and variable production are included in operating expenses. Whatever the project's efficiency, there are always fixed costs: labour, overhead, maintenance, insurance, taxes, rent, and environmental fees [24]. On the contrary, variable costs are contingent upon production rate and output. These expenses include raw materials (such as ethanol, RSO, and potassium hydroxide), utilities (such as energy, water for heating and cooling, and transportation), packaging, and disposal of waste (such potassium phosphate). Overall variable costs can be decreased by making effective use of resources, such as reducing raw material losses and energy consumption [35]. Because they are so expensive, raw materials make up a large amount of the cost of production. The labour cost estimate for the factory was USD 64,512, taking into account six (6) operators working eight-hour shifts each day for 48 weeks at a rate of USD 20 per hour, with three operators per operator and one supervisor (at a labour cost of 25% overall).

#### 4.3. Economic Viability Indicators

Sales of the investment's products, including both the primary output and any byproducts, generate income. In this instance, the created glycerin was judged to be worth credits. Gross margin, which is determined by deducting the cost of raw materials from product sales revenues, is another crucial metric for assessing economic viability. Beyond production costs, the retained revenues are revealed by the gross margin. The cash cost of production (CCOP) is subtracted from biodiesel revenues to determine profit. This profit is known as the gross profit, from which the net profit is calculated by subtracting the corporate tax, which was calculated in this study to be 22.5%. Equation (29), when applied, yields the tax amount.

As indicated by Equation (29), the simple payback is computed by dividing the fixed investment by the average annual cash flow, which should only comprise revenue-generating years 1 through 15.

As long as it is included in the range of revenue-generating years, working capital is not included in the average cash flow calculation.

$$\text{Tax Paid} = \text{Taxable Income} \times \text{Tax Rate} \quad (29)$$

where taxable income is Total Income—Deductions—Exemptions

$$\text{Pay - back time} = \frac{\text{Total Investment}}{\text{Average annual cash flow}} \quad (30)$$

Depreciation charges are computed using the decreasing balance depreciation method in situations where cash flow is predominant. In this research, a depreciation rate of 10% was considered throughout a project lifetime of 15 years, with a 5-year project recovery phase. The return on investment (ROI) is determined by deducting expenditures from income, and the resultant amount is known as the net profit. Both the HC and MS procedures have a 15-year recovery period, which reflects the project's economic viability [24]. However, an 11% discount rate was proposed in this study. The economic statistic known as the net current value (NPV) estimates the difference between the current values of cash inflows and outflows [45]. The annualization of an interest rate is used to account for the time worth of money. Equation (31) is used to compute the NPV.

$$NPV = \sum_n \frac{C_t}{(1+r)^n} - C_o \quad (31)$$

where  $C_t$  and  $C_o$  are the net cash inflow and initial investment costs, respectively,  $n$  = projects lifespan, and  $r$  = discount rate

In other words, a high-percentage ROI indicates a comparable investment's returns relative to its costs. The return on investment, or ROI, is computed as the ratio between net income and investment. Thus, it is a metric for evaluating the effectiveness of investments and may be applied to compare the relative performance efficiencies of many expenditures. Equation (32) provides an additional definition for ROI.

$$ROI = \frac{C_{NET}}{n + C_o} \quad (32)$$

where  $C_{NET}$  and  $C_o$  are the cumulative net profit and initial investment costs, respectively, and  $n$  is the plant life.

#### 4.4. Environmental Analysis

Environmental effects, especially those related to greenhouse gas emissions and carbon footprint, must be taken into account for the new procedure under consideration. The carbon footprint, commonly expressed as kgCO<sub>2</sub> eq, is a measure of the amount of greenhouse gases released per unit of product. During the production of biodiesel, energy consumption contributes significantly to greenhouse gas emissions. The MS method employs energy for preheating, ethanol recovery, and biodiesel distillation, including the utilization of a high-duty steam boiler, whereas the HC process mainly relies on energy for raw material preheating. This study examined the production of steam for heating and the consumption of electricity as the two primary sources of CO<sub>2</sub> emissions. Equation (33) illustrates the specific equation that was used to determine the CO<sub>2</sub> emissions from energy usage.

$$Q_E CO_2 = CW_{el} * SW_{el} \quad (33)$$

$CW_{el}$  represents electricity consumption and  $SW_{el}$  denotes the electricity supplier identified emission factor (given as 438.64 g CO<sub>2</sub> eq/kWh [45]).

The emission resulting from the creation of steam can be calculated using Equation (34), assuming that the boiler (steam generator) is powered by natural gas.

$$T_E CO_2 = Q_F * \dot{E}_S * F_{CO_2} \quad (34)$$

where  $Q_F$  is the fuel quantity,  $\dot{E}_S$  is energy per unit mass associated with steam production (0.0471 GJ/kg), and  $F_{CO_2}$  is the carbon equivalent per unit energy emitted (0.05582 t CO<sub>2</sub>/GJ [46]).

## 5. Results and Discussion

### 5.1. Production Process of *Hevea brasiliensis* Ethyl Ester

Figure 2 depicts an integrated production plant for producing MS and HC based biodiesel, demonstrating how the reactants are treated equally in both processes with respect to pressure, temperature, composition, flow rates, and molar ratio before reaching the transesterification reactor step. Reaction stoichiometry is used to maintain the alcohol to oil molar ratio at 3:1.

*Hevea brasiliensis* ethyl ester from rubber trees produces excellent biodiesel. It avoids food competition, is perennial, and produces a great amount of latex. In addition, it is climate-adaptable, has a lower carbon intensity, and contributes to emission reduction. The HCR and the MSR systems produce biodiesel at a mass flow rate of 9325 kg/h and 8625 kg/h, respectively, with the former reaching a purity that is about 5% higher than the latter. This is because the HCR delivers higher product purity and conversion than the MSR. Similar findings were reported by Gholami et al. [22], where the HCR produced biodiesel with a 9.6% greater purity than the MSR.

Biodiesel is primarily combined with residues and traces from unconverted RSO in the Splitter-1 overhead of the MS process. This mixed stream is created in a vacuum distillation column to yield pure biodiesel (>99%). The HC technique eliminates the need for a column, saving energy and money. This 10-stage column has a reflux ratio of 2, with vacuum pressures of 0.2 and 0.1 bar in the reboiler and condenser, respectively. To separate the hydrophobic and hydrophilic phases that occur during the emulsion of glycerol and biodiesel, water washing is utilized. Potassium-hydroxide-containing waste streams

(11 and 16 for MS and HC, respectively) are neutralized and transformed into potassium phosphate. The HC reactor uses cavitation processes to produce high-intensity cavitation, whereas the CSTR uses a mechanical agitator that consumes a large amount of energy (88.24 kW). The HC reactor uses cavitation processes to produce a high-intensity cavitation of 0.313 [22], whereas the CSTR requires a mechanical agitator that consumes a large amount of energy (88.24 kW). Consequently, the contact surface area increased, resulting in greater productivity and conversion as compared to the stirred tank reactor. This phenomenal increase in contact surface area results in a reduction in the mass transfer resistance and almost full conversion in a brief residence time. Thus, the HC process outperformed the MS stirred tank reactor process in terms of conversion and productivity.

### 5.2. Energy and Exergy Discussion

Mass, energy, and energy flow analysis provide a way to evaluate operations and are invaluable tools for determining material losses, waste, energy loss, and irreversibility. Assessing a system's energy and energy efficiency helps to pinpoint areas that need to be improved. Exergy is a useful metric for gauging material reactions and energy quality, as well as for identifying renewable energy sources and processes. Mass, energy, and exergy are evaluated for a variety of chemical components, including mixes and utility systems, as part of the analysis. The study includes the overall process exergy, which is calculated by summing the input/output chemical and physical exergy of the constituents in the process streams (see Table 3). Standard values are used for other substances such as phosphoric acid, potassium phosphate, potassium hydroxide, and ethanol. The Gibbs free energy of the formation and chemical exergy of the glycerides, fatty acids, and biodiesel are evaluated by adopting an assumed average molecular weight for the acids and ethyl carbon chains in the reaction process. Appendix Table A2 gives the findings of the thermodynamic study for the streams used in the production processes of biodiesel in the MSR and HCR. Tables 3 and 4 present the exergetic destruction, exergetic fuel depletion, exergetic efficiency, and exergy improvement potential of each component of the two processes, respectively. These can be seen as percentage irreversibility ratios,  $y^* D$ , and exergetic destruction.

The ease of installation, easy of scaling up, and simple configuration of the HC process (see Appendix Figures A1 and A2) provide a clear advantage over the MS process in the comparison of the two process scenarios. There was a 99.01% conversion rate set for both processes in the model configuration and conditions. The HC system, however, offers higher conversion rates than the MS method, as confirmed by the sensitivity analysis, which is a component of the simulation findings. The emulsion effect created in the HC reactor, which improves the contact between the oil and alcohol phases, may be responsible for the HC process's higher conversion rate. As shown in Figure 2, the MS design has 94.85% recovery and 88.24 kW energy consumption at the same reactor volume of 15 m<sup>3</sup> for both processes, whereas the HC reactor achieves a conversion rate of 99.01% and uses only 2.274 kW.

**Table 3.** Exergetic data of streams for the HC process.

Component	Fuel Exergy EX <sub>FUEL</sub> [MW]	Product Exergy EX <sub>PROD.</sub> [MW]	Destroyed Exergy EX <sub>DESTROYED</sub> [MW]	Exergy Destruction [%]	Exergetic Fuel Depletion Ratio, y <sub>D</sub>	Irreversibility Ratio, y*D [%]	Exergy Efficiency [%]	Improvement Potential [MW]
Pump-1	0.00	0.00	0.00	99.56	0.00	0.08	0.44	0.00
Pump-2	0.00	0.00	0.00	99.99	0.00	0.38	0.01	0.00
Heater	97.10	97.10	0.00	0.00	0.00	0.05	100.00	0.00
Splitter-3	108.41	108.41	0.00	0.00	0.00	0.02	100.00	0.00
Splitter-4	4.76	4.53	0.23	5.09	0.21	92.48	95.15	0.01
Reactor-2	108.42	108.40	0.02	0.01	0.01	6.19	99.99	0.00
Washing-RXR	4.53	4.53	0.00	0.03	0.00	0.50	99.97	0.00
Valve	108.42	108.42	0.00	0.00	0.00	0.30	100.00	0.00
Total	108.42	97.10	0.25	0.23	0.23	100.00	89.56	0.03

**Table 4.** Exergetic data of streams for the MS process.

Component	Fuel Exergy EX <sub>FUEL</sub> [MW]	Product Exergy EX <sub>PROD.</sub> [MW]	Destroyed Exergy EX <sub>DESTROYED</sub> [MW]	Exergy Destruction [%]	Exergetic Fuel Depletion Ratio, y <sub>D</sub>	Irreversibility Ratio, y*D [%]	Exergy Efficiency [%]	Improvement Potential [MW]
Pump-1	0.00	0.00	0.00	99.56	0.00	0.01	0.44	0.00
Pump-2	0.00	0.00	0.00	99.99	0.00	0.05	0.01	0.00
Comp	0.01	0.01	0.00	7.60	0.00	0.06	92.40	0.00
Heater	97.10	97.10	0.00	0.00	0.00	0.01	100.00	0.00
Splitter-1	109.69	109.69	0.00	0.00	0.00	0.00	100.00	0.00
Splitter-2	5.44	4.76	0.68	12.42	0.31	38.05	87.58	0.08
Reactor-1	109.76	109.68	0.08	0.08	0.04	4.72	99.92	0.00
Catalyst-RXR	5.44	4.53	0.91	16.66	0.42	51.05	83.34	0.15
Column	106.86	106.76	0.11	0.10	0.05	6.04	99.90	0.00
Total	216.64	118.98	1.77	0.82	0.82	100.00	54.92	0.80

Figure 3 portrays that the volumetric deviation drops when the conversion rates of the MS and HC processes increase and decrease, respectively. In other words, the PFR of the HC process benefits from a lower volumetric reactor than the CSTR of the MS process. Furthermore, Chuah et al. [47] used an orifice plate with 21 holes of 1 mm diameter to produce a cavitation number of 0.3 in contrast to this investigation. In comparison to mechanical stirring for the methyl ester synthesis process, their results demonstrated an eight-fold increase in yield efficiency and a six-fold reduction in reaction time. The designed HC table system in an ethyl ester production system was validated in our investigation with a cavitation number of 0.313 achieved with a throttling valve and a PFR. Using the same reactants, Ahmad et al. [48] obtained a 98% conversion rate; however, the HC reactor in our investigation achieved a high conversion rate of 99.01%, negating the requirement for a distillation column to separate the generated oil and ethanol from the biodiesel. Lowering downstream units lowers production and capital expenses. Similar to this, Gholami et al. [22] used a constructed cavitation chamber with a cavitation value range of 0.23 to 0.64 through several cavitation zones to achieve a conversion rate of 99.9%.

On the other hand, as seen in Tables 4 and 5, the exergy balances were carried out to evaluate the material and energy-saving potential of the HC and MS processes and compare their performance. Exergetic efficiency and exergy destruction are quantified in Tables 4 and 5, respectively, by analyzing the exergy flow for the HC and MS processes in order to identify waste streams. Oil accounts for the bulk of input exergy (82.92%) in the MS process, whereas biodiesel yields the largest exergy output (80.8%). Waste streams total 12.6% and include unreacted oil (6.6%), ethanol–water–biodiesel mixture, and ethanol–water mixture. Similar to the MS, the HC process shows oil as the primary exergy input (82.92%), but no significant waste streams are observed compared to the MS process. Overall, the processes delivered a mass flow rate of 9325 kg/h and 8629 kg/h of biodiesel from the HC and MS systems, respectively. After all equipment irreversibility rates were assessed, the overall exergy efficiency for the MS process was 54.92%, while the HC process's was 89.56%.

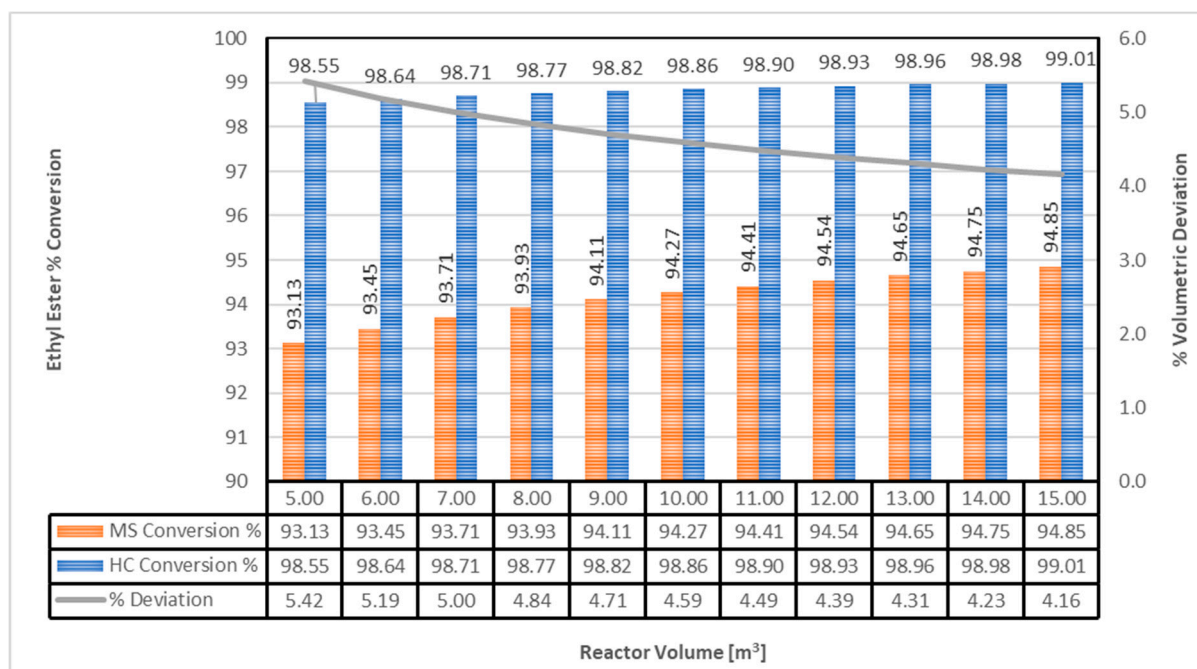


Figure 3. Conversion rate comparison (sensitivity assessment curve).

Table 5. Summary of total capital investment and total production cost [24].

Cost Parameter	Cost of MS Plant (USD)	Cost of HC Plant (USD)
I. Fixed Capital Investment (DC + IC)	12,295,681.44	8,642,910.43
A. Direct costs (DC)	10,691,896.90	7,202,425.36
1. Onsite (ISBL) cost	8,224,536.08	5,540,327.20
2. Offsite (OSBL) cost (30% of ISBL)	2,467,360.82	1,662,098.16
B. Indirect costs (IC)	1,603,784.54	1,440,485.07
1. Engineering and supervision (5% of DC)	534,594.85	360,121.27
2. Contingencies (10% & 15% of DC)	1,069,189.69	1,080,363.80
II. Other Outlays (OO)		
A. Startup costs (10% of DC)	1,069,189.69	720,242.54
B. Working capital (15% of DC)	2,084,919.90	1,458,491.14
Total capital investment	14,380,601.34	10,101,401.57
Raw materials Cost		
Rubber seed oil (86.5 ton)	196,787.50	196,787.50
Ethanol (13.5)	6750.00	6750.00
Potassium hydroxide (0.53 ton)	307.40	307.40
Phosphoric acid (0.2 ton)	167.45	167.45
Utilities		
Steam (0.0227/MJ)	9368.56	393.19
Variable production cost/day	213,380.91	204,405.54
A. Direct production costs		
1. Labour (%)	64,512.00	64,512.00
a. Number of Labour (8)	30,720.00	30,720.00
b. Supervision (25% of operating labour).	15,360.00	15,360.00
c. Direct salary overhead (40% of (a+b))	18,432.00	18,432.00
2. Repair and maintenance (2%)	4267.62	4088.11
3. Packing (2%)	4267.62	4088.11
4. Waste stream disposal (1%)	2133.81	2044.06
B. Fixed charges		
1. Depreciation (10%)	21,338.09	20,440.55
Annual Production Summary		
Total Fuel produced/day	207.00	224.00
Total production cost/day	288,561.96	279,137.81
Plant uptime for 7920 Hrs (90.4%)		
Total production cost/yr at Uptime	95,213,903.67	92,104,312.95
Gross Profit/d	320,850.00	347,200.00
Gross Profit/yr @ uptime	105,867,666.00	114,562,112.00
Net Profit Per year	10,653,762.33	22,457,799.05

Market price of biodiesel is 1550 USD/t, RBO is 2.275 USD/kg, ethanol is 0.5 USD/kg, KOH is 0.58 USD/kg, and H<sub>3</sub>PO<sub>4</sub> is 0.85 USD/kg.

### 5.2.1. Exergy Destruction

By comparing the exergy destruction in each component to the total exergy destruction of the process, the ratio is  $y_{D,i}^*$  and the exergy destruction ratio is  $Ex_{D, Tot}$ . The exergy destruction and efficiencies of each part of the two processes are shown in Tables 4 and 5. The values of exergy destruction for the HC and MS processes were found to be 0.25 MW and 1.77 MW, respectively. This suggests that, in comparison to the MS process, the HC process has about a sixth of the energy destruction. Analysis of the MS process's components revealed that, as shown in Figure 4, the phases of glycerin purification and catalytic removal contributed the most exergy destruction, at roughly 51% and 38%, respectively. In other words, both components contributed about 89% to the irreversibility ratio of the MS system. Additionally, it is shown that both components have improvement potentials of 0.08 MW and 0.15 MW, respectively, suggesting that by giving their designs the attention they need, these components might be made better and more effective. Conversely, the glycerin recovery (Splitter-4) unit, like the MS process, only contributed 93% exergetic degradation to the irreversibility of the system. In general, the exergetic destruction of the HC process is shown in Figure 5. Only a careful design is needed to maximize the component's exergetic improvement ratio of 0.01 MW.

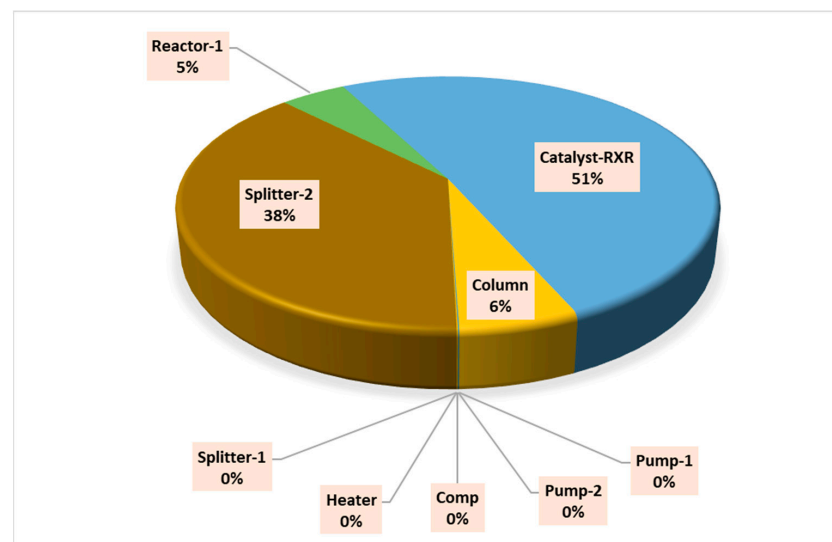


Figure 4. Components' exergetic destruction in the MS conversion process.

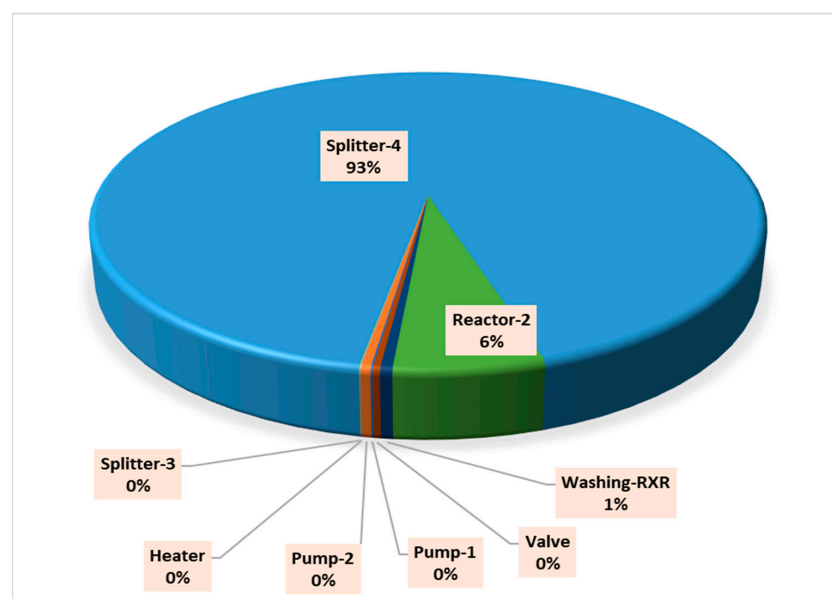


Figure 5. Components' exergetic destruction in the HC conversion process.

Reducing energy destruction in this stage has been achieved by using the solvent washing and decanting process to separate the phases of oil and biodiesel. However, the HC method has a significant advantage over the MS process in that it does away with the requirement for the biodiesel purification step because of its high conversion efficiency. Exergy destruction is largely attributed to the transesterification reactor, which comes after the biodiesel purification stage. The HC process exhibits around 8% less exergy destruction than the MS process. As compared to the MS process, the HC method uses only 3% of the electrical power in the reactor, demonstrating lower energy use. This reduction can be justified by the shorter reaction time and optimum mixture that cavitation produced at the microscopic level. The transesterification stage of ethanol recovery adds to the MS process's exergy destruction, but the HC process has less exergy destruction because less alcohol needs to be separated and it is not recycled.

Since the HC process requires a mixer to be present before the reactor, the MS method's mixing stage has a significantly lower energy destruction. The variation in reaction conditions, specifically in temperature and pressure, also affects the rates of energy destruction. As the HC process operates at room temperature and does not require preheating, there is no exergy destruction during this stage.

### 5.2.2. Exergy Efficiency

The energy and exergy efficiency of the systems' separate parts as well as the overall operations are presented in Figures 6 and 7. Tables 4 and 5 show that the HC process had the highest exergy efficiency, outperforming the MS process by over 35%. This was because the HC process had a greater conversion rate in the reactor and reduced waste emissions and exergy destruction. The exergy efficiencies of the major model components were generated and are displayed in Figures 6 and 7 for the MS and HC systems, respectively. The total input exergy for both processes was 108.64 MW and 216.64 MW. Despite being the stage that contributes the most to energy destruction, the catalytic removal stage demonstrated a notably high exergy efficiency because of the significant fuel exergy input and conservation in the MS process's product stream. The HC process, on the other hand, contributed the second most to energy destruction. On the other hand, as shown in Figures 6 and 7, the biodiesel pumps had the lowest exergetic efficiency because of the large pressure differential that the pump creates and the mass flow rates that result in increased pump shaft power.

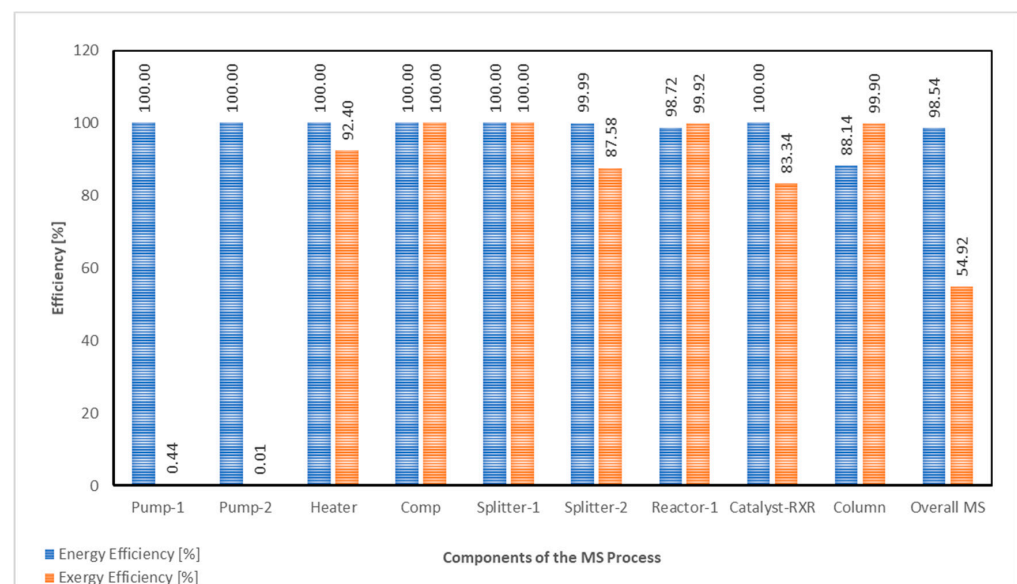


**Figure 6.** Components' exergetic efficiency in the MS conversion process.

For obvious reasons, the HC process does not require the column; however, this model has noted that the distillation column for the MS process requires a significant amount of steam. It has been shown that steam injected at the column accounts for approximately 49% of the fuel exergy input in the MS process. Despite the huge fuel contribution, the exergetic efficiency ranked amongst the highest in the system. This aligns reasonably well with a previous study by Blanco-Marigorta et al. [49].

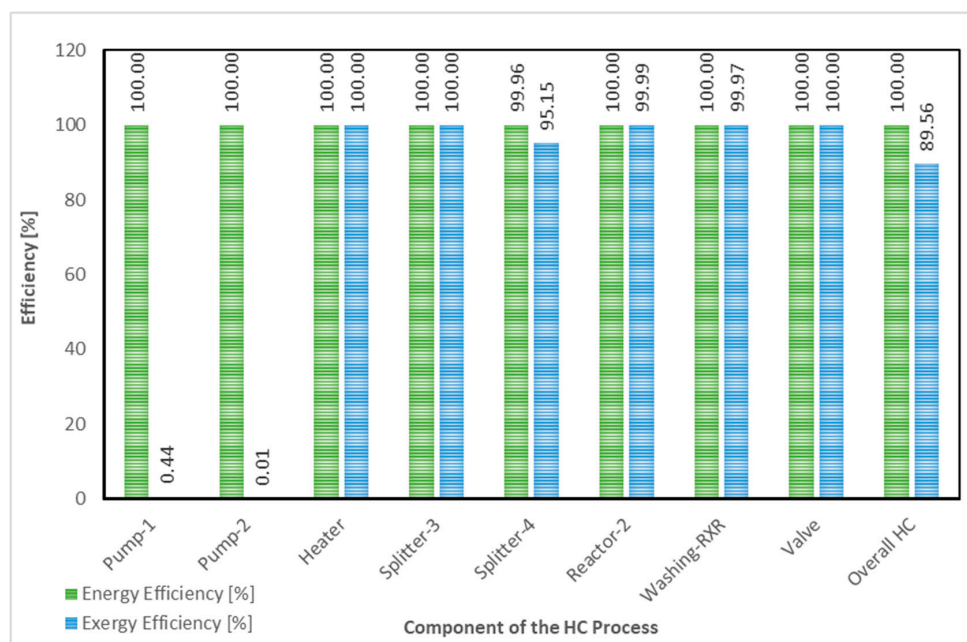


**Figure 7.** Components exergetic efficiency in the HC conversion process.

A notable discrepancy was noted in the transesterification phase, when the exergy efficiency of the reactor exceeded 99% in the current study, in contrast to 69% in Blanco-Marigorta et al.'s study [49] and 98% in Gholami et al.'s study [22].

This discrepancy might be ascribed to the differences in chemical exergy between rubber seed oil, canola oil, and jatropha oil employed in the several studies listed for the production of biodiesel. Even when converted 100%, the biodiesel produced from jatropha and canola oil appears to have a larger chemical exergy, which leads to a lower exergy efficiency. However, as can be seen in Figures 6 and 7 for reactors 1 and 2, respectively, RSO and its biodiesel show comparable chemical exergies that allow for a higher exergy efficiency of up to 99.9% at complete conversion. This demonstrates that, in terms of exergy efficiency, RSO is a more advantageous fuel for the manufacture of biodiesel. An essential factor in determining whether biodiesel production can be sustained in place of fossil fuels is how renewable it is in terms of energy.

The generation of ethanol and biodiesel from different feedstocks was studied in a study by Velasquez et al. [50], and their renewability performance was measured using an exergy-based indicator. The results showed that biodiesel production exhibited a renewable process with an efficiency of 74.7% and a high exergy content per unit of dried biomass. In light of this, the research indicates that producing biodiesel has the potential to be a renewable process. It also shows that the transesterification step can achieve exergy efficiencies exceeding 99%, mainly because the products have a high exergy content and low exergy destruction. Utilizing hydrodynamic cavitation processes improves production efficiency in biodiesel facilities by reducing waste emissions and exergy destruction as compared to mechanical stirring. It is interesting, however, that of all the steps of biodiesel production, the transesterification stage has one of the lowest exergy destructions. Thus, new advancements like plant species identification should be taken into consideration in order to further limit energy destruction in the biodiesel life cycle.

## 6. Economic Assessment

The manufacturers base their investment strategy primarily on the total cost of capital investment, with special attention to the ISBL plant cost as the most important consideration at first. Table 5 shows that the ISBL cost for the MS process was USD 8,224,536.08, whereas the HC process produced an ISBL cost of USD 5,540,327.20 using the Bridgewater's technique. The plant cost of the HC plant is approximately 1.4 times less than the plant cost of the MS plant. The MS plant's costly distillation equipment, which is necessary to separate biodiesel from unconverted rubber seed oil, is the main cause of this cost difference. The substantial divergence in investment costs indicates a promising outlook for industrial HC plants in biodiesel production. Similarly, Innocenzi and Prisciandaro [51] came to a comparable conclusion, pointing out that an HC plant's ISBL cost is 1.1 times more than that of a typical biodiesel production facility.

Regarding energy consumption, the HC method is also more appealing because it uses just 17,321 MJ/d as opposed to the MS process's 412,712 MJ/d, as shown in Table 5. As a result, the MS process's increased energy consumption is mostly caused by the addition of the energy-intensive distillation unit. This significant variation in energy use supports the HC method's superior sustainability and environmental friendliness over the MS process, in line with SDG No. 12 [52] on responsible consumption and production [53]. This SDG gives attention to maximizing efficiency and output while minimizing resources. Under this framework, the proposed HC process exhibits lower energy usage and reduced losses. When evaluating a process's viability, the total production cost is just as important as the ISBL cost. For instance, Table 5 shows that the combined cost of production for both the MS and HC procedures for biodiesel is USD 1550 per ton.

However, roughly 224 tons and 207 tons of biodiesel were converted in the HC and MS procedures, respectively, for the same quantity of materials used in the biodiesel production methods. This suggests that the HC process's production costs are approximately 9.2% greater than the MS process's. Gholami et al. [22] found a similar result and noted that the MS procedure resulted in a 10% greater cost of producing biodiesel. Notably, energy expenses make up 4.4% of the variable production cost in the MS process but only 0.2% in the HC process. The analysis includes initial cash outflows for engineering costs, equipment procurement, and plant construction. The plant's cash inflows come from product sales as soon as it is operating. The estimated cumulative net cash flow over the project's 15-year lifespan is shown in a cash flow diagram, like the one in Figure 8.

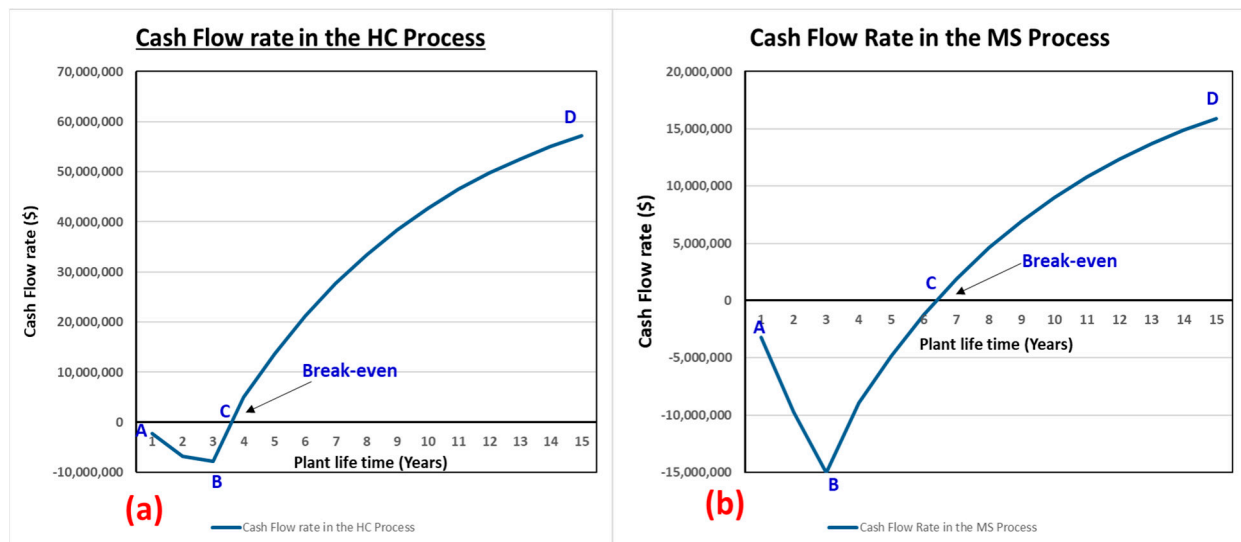


Figure 8. (a) Cash flow rate of the HC, and (b) MS process plants.

This diagram provides a clear overview of resource requirements and the timing of earnings. The design investment phase, the large capital outflow during building and startup, and the working capital, which is shown below the horizontal axis point ABC, are the distinct sections that make up the diagram. The cash flow curve turns upward toward point C when the process is operational and generates income from sales, resulting in positive net cash flow until the break-even point is reached at point C. The ascending curve all the way to point D demonstrates a positive trajectory in cumulative cash flow, indicating that the project is generating returns on investment.

The net present value (NPV) represents the difference between the present value of cash inflows and cash outflows over a specific period (in this study, 15 years). Establishing a process's economic feasibility requires a positive net present value. Appendix Tables A3 and A4 provide detailed economic analysis, whereas Table 6 summarizes the NPV for the MS and HC procedures, respectively. Year 1 of this study is the start of cash flow and is regarded as the design phase. The project receives its full fixed capital investment during the construction and installation phases of Year 2. Depreciation charges are subtracted from the gross profit once the unit reaches full capacity in Year 3. Positive NPV and return on investment (ROI) are shown for the MS and HC processes in Table 6. The MS process has an NPV of USD 15.9 million and an ROI of 55.51%, demonstrating that the investment is both feasible and profitable. On the contrary, the HC process has an ROI of 176.84% and an NPV of USD 57.2 million. Given that expenses have already exceeded

revenues, this suggests that both procedures are commercially feasible. However, the higher ROI and lower NPV of the HC procedure make it clear that it is more profitable.

**Table 6.** Economic analysis summary.

Revenues and Production Costs	HC Process	MS Process
Product revenue [USD]	114,562,112.00	105,867,666.00
Variable cost of production (VCOP) [USD]	69,469,020.42	72,519,380.83
Fixed cost of Production (FCOP) [USD]	22,635,292.66	22,694,522.96
<b>Economic analysis</b>		
Average cash flow /year [USD]	17,805,196.54	8,545,148.81
Simple pay-back period [years]	0.57	1.68
Return on investment (15 yrs)	176.84%	55.51%
NPV (@ 15 years) [USD]	57,165,105.59	15,881,434.94
NPV to year [yrs]	4	7
IRR [%]	88.99	33.03

## 7. Environmental Assessment

Environmental effects of RSO biodiesel production include greenhouse gas (GHG) emissions, primarily CO<sub>2</sub>. Despite these emissions, biodiesel from rubber seeds is seen as a renewable fuel with lower net CO<sub>2</sub> emissions than fossil fuels. This is because it is assumed that the CO<sub>2</sub> that rubber trees absorb during growth will balance the CO<sub>2</sub> released during combustion. However, the energy used in the processes involved in the production of biodiesel has a substantial impact on the environment. Thus, it is assumed that the use of renewable energy sources can notably reduce the environmental impact associated with energy use in biodiesel production. The carbon footprint of the HC process was estimated and contrasted with that of the MS process in order to determine whether the projected biodiesel production procedure could be implemented on a large scale, as shown in Table 7.

**Table 7.** Carbon footprint of biodiesel production using HC and MS approaches.

CO <sub>2</sub> Emissions (t CO <sub>2</sub> eq./year)	MS Process	HC Process
Steam	172.7	7.24

It is worth noting that this study did not consider emissions from plant construction materials such as steel, stainless steel, and raw materials, or other life cycle assessments (LCAs). This study focused mainly on electricity and thermal energy emissions relating to biodiesel production. Specifically, the emissions resulting from steam consumption were found to be 172 t CO<sub>2</sub> eq./year for the MS process and only 7.2 t CO<sub>2</sub> eq./year for the HC process. This significant difference indicates that the HC process generates approximately 24 times fewer CO<sub>2</sub> emissions than the MS process, affirming its position as a cleaner and more environmentally sustainable production pathway. It may also be relevant to exergy waste emission in relation to the environment in the production of biodiesel. In this study, the MS process resulted in a substantial waste of 5.52 MW of exergy, with a significant proportion of approximately 82% stemming from the unreacted oil present in the bottom stream of the biodiesel purification tower. Conversely, the HC process exhibits a significantly lower exergy waste emission of 1.12 MW, reflecting a reduction of 78%. Notably, this is due to the efficient conversion in the reactor and lower consumption of alcohol and oil, providing a notable improvement compared to the MS process.

In this study, the comparison of HC and MS reactors for RSO biodiesel production has been expansively discussed from varying points of view. HC proves more viable due to specific factors. HC relies on fluid flow for cavitation energy, requiring minimal additional energy, while MS needs continuous energy input from motors, making HC more energy-efficient, especially in large-scale applications. HC has fewer parts, leading to lower maintenance and less wear. It enables process intensification, speeding up reactions. Additionally, HC is environmentally friendly, reducing the need for chemicals and aligning with green chemistry practices, whereas MS emits more carbons.

MS reactors are versatile and widely adaptable to different reaction conditions in various industries relative to HC reactors. They are also easily scalable and hence suitable for both small-scale and large-scale biodiesel production. Finally, MS reactors provide uniform mixing for all reactants to ensure consistent product quality in many biodiesel production facilities.

## 8. Conclusions

This passage discusses the increasing interest in advanced transesterification reactors for biodiesel production, driven by the need for cost efficiency, enhanced biodiesel quality, faster reactions, and environmental benefits. However, challenges like high construction costs and energy management hinder large-scale biodiesel production from RBO. The study emphasizes the necessity for affordable and versatile reactors applicable to various feedstocks, ensuring their economic and environmental viability. The research compares tube-like plug-flow reactors (PFRs) and continuous stirred tank reactors (CSTRs) for converting RSO and fats into biodiesel, analyzing their limitations and impacts. The study also explores key parameters affecting transesterification and conducts a comparison between traditional mechanical stirring (MS) and innovative hydrodynamic cavitation (HC) methods, utilizing Aspen HYSYS version 10 software for biodiesel production analysis. An exergetic analysis technique has been adopted, it being a valuable tool for designing and evaluating energy systems and assessing the efficiencies of energy components. This methodology proves its practicality in improving energy and exergy efficiency in the production process of biodiesel from ethyl ester. The main conclusions are as follows:

- Biodiesel production processes showed energy efficiencies of 98.54% for MS and 100% for HC, with exergy efficiencies of 54.92% and 89.56%, respectively.
- Exergy analysis is vital for understanding energy use in biodiesel production. MS used 88.24 kW energy for a 94.85% conversion rate, whereas HC used 2.274 kW for 99.01% conversion at the same volumetric reactor rate.
- The study quantifies inefficiencies, helping to assess component performance and develop sustainable biodiesel production. MS's exergetic destruction is six times higher than HC's.
- Chemical exergy from RBO and ethanol is the major input, while glycerol and water cause significant exergy losses in the biodiesel production process.

Suffice to say, energy efficiency is crucial in biodiesel production, and employing exergetic techniques can significantly reduce energy consumption. This approach helps industries and stakeholders to focus on energy savings when selecting reactors. By addressing components with high exergetic destruction through proper design, performance efficiency is assured, minimizing energy costs and reducing irreversibilities of the components of the systems.

Economic and environmental assessments compared MS and HC biodiesel production. The MS plant investment cost was 1.5 times higher than HC, making HC more profitable (NPV: USD 57.2 million, ROI: 176.84% vs. USD 15.9 million, ROI: 55.51% for MS). Additionally, HC emitted significantly less CO<sub>2</sub> (7.2 t CO<sub>2</sub> eq./year) compared to MS (172 tCO<sub>2</sub> eq./year) due to MS's higher energy requirements. Implementing HC not only enhances efficiency and profitability but also reduces energy consumption, material usage, and waste, promising cleaner biodiesel production and sustainable energy development.

The optimization of biodiesel production from RSO often generates unrecoverable waste. A circular economy approach is crucial for enhancing the entire production chain, maximizing resource efficiency and ensuring sustainability. Stakeholders and industry merchants play a vital role in this process, particularly through sustainable rubber plantation farming practices that maintain a steady supply of seeds without depleting natural resources. To minimize waste, exploring options like utilizing by-products such as seed husks for composting or biomass energy generation is essential. This area lacks substantial research and presents a promising future study. Engaging stakeholders actively can facilitate the biodiesel industry's shift toward a circular economy, reducing environmental impact and fostering economic growth through innovation, job creation, and resource optimization.

### *Future Research Areas*

Future research in biodiesel production via the transesterification process should focus on

1. Developing efficient and eco-friendly catalysts, exploring options like enzyme catalysts and nanocatalysts.
2. Addressing the issue of waste utilization is crucial. Research should investigate methods to utilize waste materials, such as finding uses for glycerol by-products and developing more efficient purification techniques to reduce overall waste.
3. Lastly, comprehensive life cycle assessments (LCAs) can evaluate the environmental impact of biodiesel production, guiding decision making toward more sustainable practices.

**Author Contributions:** Conceptualization and writing—review and editing, O.D.S. and P.A.A.; methodology, T.K.T.; software and formal analysis, H.F.; data curation and validation, C.P. and O.D.; formal analysis and writing—review and editing; A.E. and C.C.E.; writing—original draft preparation, A.M. All authors have read and agreed to the published version of the manuscript.

**Funding:** This research received no external funding.

**Institutional Review Board Statement:** Not applicable.

**Informed Consent Statement:** Not applicable.

**Data Availability Statement:** Data are contained within the article.

**Conflicts of Interest:** The authors declare no conflict of interest.

### Nomenclature

BD	Biodiesel
CC	Contingency cost
CCPP	Combined cycle power plant
CV	Control volume
CSTR	Continuously stirred tank reactor
EC	Engineering cost
ER	Ethylic routes
FAME	Fatty acid methyl ester
FCI	Fixed capital investment
GLC	Glycerol
GWP	Global warming potential
HC(R)	Hydrodynamic cavitation reactor
HEP	Hydroelectric power
HHV	Higher heating value (MJ/kg)
IR	Interest rate
IRR	Internal rate of return
ISBL	Inside battery limit
MACRS	Modified accelerated cost recovery system
ME	Methylic route
MS(R)	Mechanical stirring reactor
NCGOs	Non-competitive generational oils
NPV	Net present value
NRTL	Nonrandom two liquid
OPEX	Operating expenditure
OSBL	Outside battery limit
PCE	Purchase cost of equipment
PFR	Plug flow reactor
PPC	Physical plant cost
ROI	Return on investment
RSO	Rubber seed oil
SDG	Sustainable development goal
TC	Total production cost
TCI	Total capital investment
TEA	Techno-economic analysis
TFC	Total fixed cost
TG	Triglyceride
TPC	Total production cost
TVC	Total variable cost
UNFCCC	United Nations Framework Convention on Climate Change
WCI	Working capital investment

**Greek letters**

$\varphi$	coefficient from the liquid fuel expression
$\eta_{\dot{E}}$	energy efficiency
$\eta_{ex}$	exergy efficiency
$\eta_{Pump}$	pump efficiency
$\eta_{th}$	thermal efficiency

**Abbreviations**

$\dot{E}$	energy rate [kW]
Ex	exergy rate [kW]
ex	specific exergy rate of material streams (kJ/kmol)
Ex <sub>D</sub>	exergy destruction rate
Ex <sub>L</sub>	exergy loss rate
W <sub>Net</sub>	net power (kW)
W <sub>P</sub>	pump power (kW)
y <sub>D</sub>	exergy destruction rate ratio
h <sub>i</sub>	specific enthalpy at initial state (kJ/kmol)
h <sub>o</sub>	specific enthalpy at reference state (kJ/kmol)
KE	kinetic energy
LHV	lower heating value (MJ/kg)
$\dot{m}$	mass flow rate [kg/sec]
$\dot{m}_{Fuel}$	mass flow rate of Fuel [kg/sec]
P	power output [kW]
P <sub>o</sub>	pressure at reference state (atm)
PE	potential energy
Q	heat flow rate
S <sub>i</sub>	specific entropy at initial state (kJ/kmol)
S <sub>o</sub>	specific enthalpy at reference state (kJ/kmol)
T <sub>o</sub>	temperature of reference state (K)

**Subscripts**

CHM	Chemical
D	Destruction
F	Fuel
In	Inlet streams
K	kth component of system
O	Reference state
O	Ambient
Out	Outlet stream
P	Product
PHY	Physical
Th	Thermal
Tot	Total

## Appendix A

**Table A1.** An overview of techno-economic scrutiny of biodiesels derived from oily feedstocks.

Reactor Technology	Source	Types of Alcohol Methanol	Ethanol	E <sub>a</sub>	TE <sub>a</sub>	Technological Challenges	Remarks	Refs.
LSC	Rice bran oil (RBAO)	✗	✓	✓	✓	The cost of lipase catalyst influenced the recovery and re-usage	The adoption of TEAs into rice bran oil refinery led to profit and a reduction in toxic chemicals and energy	Usaku et al. [54]
Sonication	Acidic oil	✓	✗	✓	✓	NS	The production cost (0.776 USD/liter), total CO <sub>2</sub> emissions (0.08 kg of CO <sub>2</sub> /kg of BD), and return of investment (~330%) obtained for the medium-sized production unit	Naeem et al. [16]
Meso-OBR	Refined and low-grade vegetable oils (RLVOs)	✓	✗	✓	✓	NR	TEAs for a single step for BD derived from RLVO established.	Al-Saadi et al. [55]
LSR	Algal biomass (AB)	✓	✗	✓	✓	The economic viability of the production of the recycle of the process	Feasibility of AB biodiesel on a large scale guaranteed	Mustapha et al. [42]
HCR		✓	✗	✓	✓	NR	Feasibility of techno-economics via Aspen version 10 software established	Oke et al. [56]
LSR	Marine macroalgae <i>Codium tomentosum</i>	✓	✗	✓	✓	NR	The payback period (8.59 yrs.) and +ve NPV (1.38 M USD/yr.) from biodiesel production (20 MT/batch) process) recorded	Gengiah et al. [57]
LSR	Palm and <i>Jatropha</i> biomass (PJB)	✓	✗	✓	✓	Attractions of TEA of hybrid of PJB for bio-refinery established	Technological bottleneck in obtaining valuable products from PJB	Niño-Villalobos et al. [58]
CSTR	<i>Calophyllum inophyllum</i> oil (CaO)	✓	✗	✗	✓	Low feedstock cost and high biodiesel conversion	Value of TEA, annual biodiesel revenue, and payback period for CaO documented	Naveenkumar and Baskar [59]
Alkali-cat, C-SCM and L-SCM	Palm oil	✓	✗	✓	✓	High amount of methanol during C-SCM process makes financial profitability realistic in the recycling loop	Financial aspect of L-SCM process ranked the best, followed by the Alkali-cat process, then the C-SCM	Sakdasri et al. [60]
Supercritical process	<i>Jatropha curcas</i> oil	✓	✗	✓	✓	NS	The cost of capital investment (9.41 million USD/yr.), manufacturing (25.39 million USD/yr), and total production (31.20 million USD/yr) reported	Yusuf, and Kamarudin [8]
Continuous stirred tank reactor (CSTR)	Canola oil	✓	✗	✓	✗	Inadequate mixing, elongated reaction period, high energy utilization	Economic sustainability of biodiesel production = f Plant capacity and prices of feedstock oils	Zhang et al. [61]
Batch Reactor	Microalgal biomass	✓	✗	✗	✓	Unsatisfactory mixing, long reaction period, high energy expended, low capability, and inflexibility	Cost-effectiveness was not checked	Lee et al. [62]

SCM = supercritical methanol; L-SCM = low methanol: oil molar ratio; Alkali-cat = alkali-catalyzed process; C-SCM = conventional SCM; NR = not reported; LSC = lab-scale reactor; TEAs = techno-economic analyses.

**Table A2.** A. Thermodynamic material streams data for the integrated (MS and HC) biodiesel process plant.

Name	Vapour Fraction	Temperature [C]	Pressure [bar]	Mass Flow [kg/s]	Molar Flow [kg-mole/s]	Mass Enthalpy [kJ/kg]	Mass Entropy [kJ/kg-C]	Heat Flow [MW]	Specific Exergy [kJ/kg]	Physical Exergy [kW]	Chemical Exergy [kW]	Exergy Total [MW]
Ethanol	0.00	25.00	1.00	0.38	0.01	6023.85	7.52	2.31	0.00	0.00	11,316.92	11.32
	0.00	25.00	1.00	0.12	0.00	8085.31	2.02	0.99	0.00	0.00	235.46	0.24
Triolein	0.00	25.00	1.00	2.46	0.00	2330.70	6.26	5.73	0.00	0.00	97,090.33	97.09
Water2	0.00	50.00	1.00	0.01	0.00	15,760.05	8.72	0.08	4.57	0.02	11.39	0.01
H3PO4	0.00	60.00	1.00	0.00	0.00	2104.98	31.37	0.00	39.66	0.09	1.99	0.00
1	0.00	25.00	1.00	0.51	0.01	6523.37	6.10	3.31	0.00	0.00	11,316.92	11.32
2	0.00	25.22	4.00	2.46	0.00	2330.31	6.26	5.73	0.00	0.00	97,090.33	97.09
3	0.00	25.19	4.00	0.51	0.01	6522.95	6.10	3.31	0.00	0.00	11,316.92	11.32
4	0.00	70.00	4.00	2.46	0.00	2248.96	6.00	5.53	5.68	13.98	97,090.33	97.10
5	0.00	61.06	4.00	2.97	0.01	2979.03	6.00	8.84	3.96	11.73	108,407.25	108.42
6	0.09	52.83	0.20	2.97	0.01	2979.03	6.00	8.84	3.71	10.99	108,407.25	108.42
7	0.00	70.69	0.20	2.97	0.01	2979.78	5.91	8.84	6.00	17.80	108,385.26	108.40
8	0.00	60.00	2.00	3.01	0.01	3032.75	5.98	9.12	3.59	10.81	109,668.60	109.68
9	1.00	60.00	2.00	0.00	0.00	5047.86	4.51	0.00	76.76	0.00	0.00	0.00
10	0.00	59.95	1.00	3.01	0.01	3045.67	5.98	9.17	3.59	10.80	109,675.56	109.69
11	0.00	60.00	1.00	0.38	0.01	7526.60	4.88	2.86	3.29	1.25	4531.92	4.53
12	1.00	60.00	1.00	0.00	0.00	13,318.17	11.48	0.00	3227.44	0.00	0.00	0.00
13	0.00	60.00	1.00	0.38	0.01	7494.28	5.04	2.86	3.50	1.34	5437.91	5.44
14	0.00	60.00	1.00	2.63	0.01	2398.73	6.17	6.31	3.64	9.58	105,143.64	105.15
15	0.00	70.57	0.20	2.97	0.01	3001.31	5.91	8.92	5.99	17.78	108,396.65	108.41
16	0.00	60.00	0.20	0.38	0.01	7568.48	4.89	2.88	3.31	1.26	4524.51	4.53
17	1.00	60.00	0.20	0.00	0.00	9866.16	0.00	0.00	374.54	0.00	0.00	0.00
18	0.00	60.00	0.20	0.38	0.01	7583.30	4.89	2.91	3.16	1.21	4527.25	4.53
19	1.00	166.29	0.10	0.04	0.00	4401.74	4.00	0.18	73.80	3.04	1283.49	1.29
20	1.00	326.19	4.00	0.04	0.00	4056.65	3.92	0.17	392.66	16.19	1283.49	1.30
Biodiesel2	0.00	60.00	0.20	2.59	0.01	2352.54	6.16	6.09	3.61	9.34	103,872.13	103.88
P-Salt	0.00	60.00	0.09	0.12	0.00	8025.29	1.95	0.99	0.29	0.04	230.68	0.23
Glycer	0.00	60.00	0.09	0.26	0.00	7370.51	6.40	1.91	4.53	1.18	4527.25	4.53
Water	0.00	50.00	1.00	0.00	0.00	15,760.05	8.72	0.05	4.57	0.01	6.96	0.01
P-Acid	0.00	60.00	1.00	0.00	0.00	2104.98	31.37	0.00	39.66	0.09	2.08	0.00
Alcohol	1.00	166.31	0.10	0.04	0.00	4401.36	4.00	0.18	73.83	3.07	1292.65	1.30
Oil	0.00	369.58	0.20	0.02	0.00	1530.01	4.52	0.03	286.51	5.46	752.80	0.76
Biodiesel1	0.00	166.31	0.10	2.57	0.01	2125.64	5.58	5.46	54.85	140.99	103,098.18	103.24
Glycerol	0.00	60.00	0.09	0.26	0.00	7270.11	6.39	1.87	4.47	1.15	4531.92	4.53
K3PO4	0.00	60.00	0.09	0.13	0.00	7952.68	2.47	0.99	1.51	0.19	230.70	0.23

**Table A3.** A. Summary of NPV for MS process.

Project Year	Cap Ex	Revenue	CCOP	Gr. Profit	Deprcn	Taxbl Inc	Tax Paid	Cash Flow	PV of CF	NPV
1	3,688,704.43	-	-	-	-	-	-	(3,688,704.43)	(3,207,569.07)	(3,207,569.07)
2	8,606,977.01	-	-	-	-	-	-	(8,606,977.01)	(6,508,111.16)	(9,715,680.23)
3	2,084,919.90	52,933,833.00	58,954,213.37	(6,020,380.37)	208,491.99	(6,228,872.36)	-	(8,105,300.27)	(5,329,366.50)	(15,045,046.73)
4	-	105,867,666.00	95,213,903.79	10,653,762.21	208,491.99	10,445,270.22	-	10,653,762.21	6,091,323.12	(8,953,723.60)
5	-	105,867,666.00	95,213,903.79	10,653,762.21	208,491.99	10,445,270.22	2,350,185.80	8,303,576.41	4,128,345.01	(4,825,378.59)
6	-	105,867,666.00	95,213,903.79	10,653,762.21	208,491.99	10,445,270.22	2,350,185.80	8,303,576.41	3,589,865.23	(1,235,513.36)
7	-	105,867,666.00	95,213,903.79	10,653,762.21	208,491.99	10,445,270.22	2,350,185.80	8,303,576.41	3,121,621.94	1,886,108.57
8	-	105,867,666.00	95,213,903.79	10,653,762.21	208,491.99	10,445,270.22	2,350,185.80	8,303,576.41	2,714,453.86	4,600,562.43
9	-	105,867,666.00	95,213,903.79	10,653,762.21	208,491.99	10,445,270.22	2,350,185.80	8,303,576.41	2,360,394.66	6,960,957.09
10	-	105,867,666.00	95,213,903.79	10,653,762.21	208,491.99	10,445,270.22	2,350,185.80	8,303,576.41	2,052,517.10	9,013,474.19

Table A3. Cont.

Project Year	Cap Ex	Revenue	CCOP	Gr. Profit	Deprcn	Taxbl Inc	Tax Paid	Cash Flow	PV of CF	NPV
11	-	105,867,666.00	95,213,903.79	10,653,762.21	208,491.99	10,445,270.22	2,350,185.80	8,303,576.41	1,784,797.47	10,798,271.66
12	-	105,867,666.00	95,213,903.79	10,653,762.21	208,491.99	10,445,270.22	2,350,185.80	8,303,576.41	1,551,997.80	12,350,269.46
13	-	105,867,666.00	95,213,903.79	10,653,762.21	-	10,653,762.21	2,350,185.80	8,303,576.41	1,349,563.31	13,699,832.77
14	-	105,867,666.00	95,213,903.79	10,653,762.21	-	10,653,762.21	2,397,096.50	8,256,665.71	1,166,903.48	14,866,736.26
15	-	105,867,666.00	95,213,903.79	10,653,762.21	-	10,653,762.21	2,397,096.50	8,256,665.71	1,014,698.68	15,881,434.94
16	-	105,867,666.00	95,213,903.79	10,653,762.21	-	10,653,762.21	2,397,096.50	8,256,665.71	882,346.68	16,763,781.62
17	-	105,867,666.00	95,213,903.79	10,653,762.21	-	10,653,762.21	2,397,096.50	8,256,665.71	767,257.98	17,531,039.60
18	-	105,867,666.00	95,213,903.79	10,653,762.21	-	10,653,762.21	2,397,096.50	8,256,665.71	667,180.85	18,198,220.46
19	-	105,867,666.00	95,213,903.79	10,653,762.21	-	10,653,762.21	2,397,096.50	8,256,665.71	580,157.26	18,778,377.72
20	(2,084,919.90)	105,867,666.00	95,213,903.79	10,653,762.21	-	10,653,762.21	2,397,096.50	10,341,585.61	631,873.77	19,410,251.49

Table A4. A. Summary of NPV for HC process.

Project Year	Cap Ex	Revenue	CCOP	Gr. Profit	Deprcn	Taxbl Inc	Tax Paid	Cash Flow	PV of CF	NPV
1	2,592,873.13	-	-	-	-	-	-	(2,592,873.13)	(2,254,672.29)	(2,254,672.29)
2	6,050,037.30	-	-	-	-	-	-	(6,050,037.30)	(4,574,697.39)	(6,829,369.68)
3	1,458,491.14	57,281,056.00	57,369,802.87	(88,746.87)	145,849.11	(234,595.98)	-	(1,547,238.00)	(1,017,334.10)	(7,846,703.78)
4	-	114,562,112.00	92,104,313.07	22,457,798.93	145,849.11	22,311,949.81	-	22,457,798.93	12,840,319.42	4,993,615.64
5	-	114,562,112.00	92,104,313.07	22,457,798.93	145,849.11	22,311,949.81	5,020,188.71	17,437,610.22	8,669,574.12	13,663,189.76
6	-	114,562,112.00	92,104,313.07	22,457,798.93	145,849.11	22,311,949.81	5,020,188.71	17,437,610.22	7,538,760.10	21,201,949.87
7	-	114,562,112.00	92,104,313.07	22,457,798.93	145,849.11	22,311,949.81	5,020,188.71	17,437,610.22	6,555,443.57	27,757,393.44
8	-	114,562,112.00	92,104,313.07	22,457,798.93	145,849.11	22,311,949.81	5,020,188.71	17,437,610.22	5,700,385.71	33,457,779.15
9	-	114,562,112.00	92,104,313.07	22,457,798.93	145,849.11	22,311,949.81	5,020,188.71	17,437,610.22	4,956,857.14	38,414,636.29
10	-	114,562,112.00	92,104,313.07	22,457,798.93	145,849.11	22,311,949.81	5,020,188.71	17,437,610.22	4,310,310.56	42,724,946.85
11	-	114,562,112.00	92,104,313.07	22,457,798.93	145,849.11	22,311,949.81	5,020,188.71	17,437,610.22	3,748,096.14	46,473,042.98
12	-	114,562,112.00	92,104,313.07	22,457,798.93	145,849.11	22,311,949.81	5,020,188.71	17,437,610.22	3,259,214.03	49,732,257.02
13	-	114,562,112.00	92,104,313.07	22,457,798.93	-	22,457,798.93	5,020,188.71	17,437,610.22	2,834,099.16	52,566,356.17
14	-	114,562,112.00	92,104,313.07	22,457,798.93	-	22,457,798.93	5,053,004.76	17,404,794.17	2,459,796.20	55,026,152.38
15	-	114,562,112.00	92,104,313.07	22,457,798.93	-	22,457,798.93	5,053,004.76	17,404,794.17	2,138,953.22	57,165,105.59
16	-	114,562,112.00	92,104,313.07	22,457,798.93	-	22,457,798.93	5,053,004.76	17,404,794.17	1,859,959.32	59,025,064.92
17	-	114,562,112.00	92,104,313.07	22,457,798.93	-	22,457,798.93	5,053,004.76	17,404,794.17	1,617,355.93	60,642,420.85
18	-	114,562,112.00	92,104,313.07	22,457,798.93	-	22,457,798.93	5,053,004.76	17,404,794.17	1,406,396.46	62,048,817.31
19	-	114,562,112.00	92,104,313.07	22,457,798.93	-	22,457,798.93	5,053,004.76	17,404,794.17	1,222,953.45	63,271,770.75
20	(1,458,491.14)	114,562,112.00	92,104,313.07	22,457,798.93	-	22,457,798.93	5,053,004.76	18,863,285.30	1,152,551.99	64,424,322.75

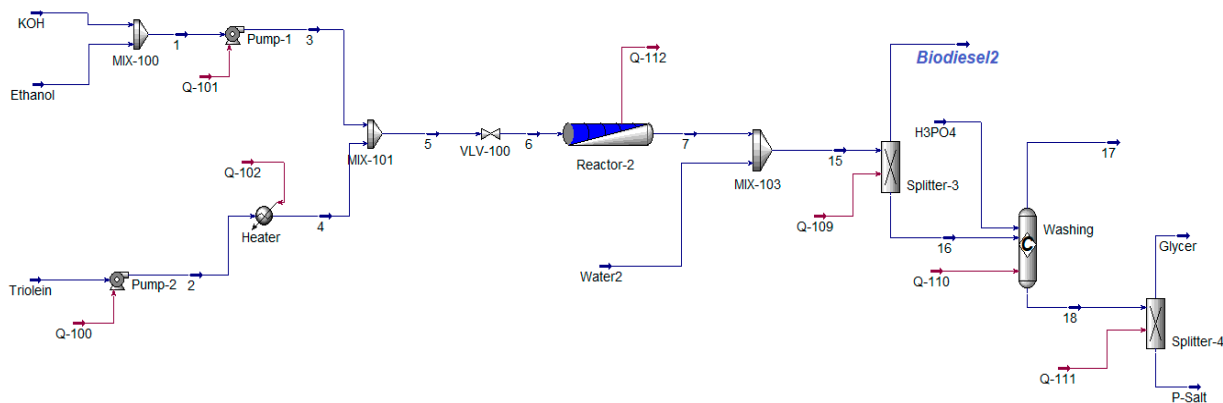


Figure A1. A. HC process feed streams simulation network.

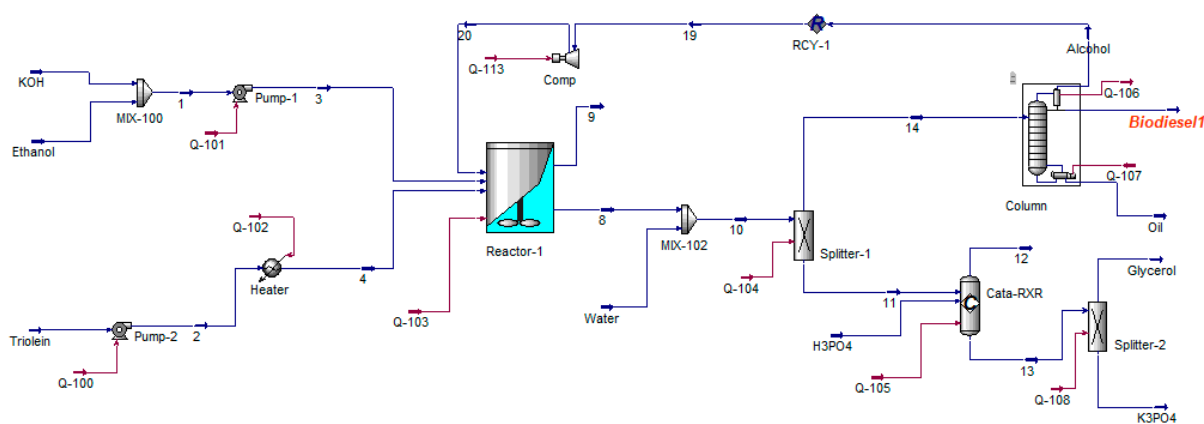


Figure A2. A. MS process feed streams simulation network.

## References

- Sajid, Z.; Khan, F.; Zhang, Y. Process simulation and life cycle analysis of biodiesel production. *Renew. Energy* **2016**, *85*, 945–952. [CrossRef]
- IEA; IRENA; UNSD; WB; WHO. *Tracking SDG 7: The Energy Progress Report 2021*; United Nations: Washington, DC, USA, 2021.
- Nhamo, G.; Nhemachena, C.; Nhamo, S.; Mjimba, V.; Savić, I. *SDG7—Ensure Access to Affordable, Reliable, Sustainable and Modern Energy*; Emerald Publishing: Bingley, UK, 2020; pp. 233–262.
- Sun, X.; Liu, S.; Manickam, S.; Tao, Y.; Yoon, J.Y.; Xuan, X. Intensification of biodiesel production by hydrodynamic cavitation: A critical review. *Renew. Sustain. Energy Rev.* **2023**, *179*, 113277. [CrossRef]
- Brahma, S.; Nath, B.; Basumatary, B.; Das, B.; Saikia, P.; Patir, K.; Basumatary, S. Biodiesel production from mixed oils: A sustainable approach towards industrial biofuel production. *Chem. Eng. J. Adv.* **2022**, *10*, 100284. [CrossRef]
- Yang, L.; Takase, M.; Zhang, M.; Zhao, T.; Wu, X. Potential non-edible oil feedstock for biodiesel production in Africa: A survey. *Renew. Sustain. Energy Rev.* **2014**, *38*, 461–477. [CrossRef]
- Samuel, O.D.; Okwu, M.O.; Amosun, S.T.; Verma, T.N.; Afolalu, S.A. Production of fatty acid ethyl esters from rubber seed oil in hydrodynamic cavitation reactor: Study of reaction parameters and some fuel properties. *Ind. Crops Prod.* **2019**, *141*, 111658. [CrossRef]
- Yusuff, A.S.; Dada, T.; Olateju, I.I.; Azeez, T.M.; Azeez, S.O. Experimental investigation of influence of methyl, ethyl and methyl-ethyl ester blends of used cooking oil on engine performances and emissions. *Energy Convers. Manag. X* **2023**, *17*, 100346. [CrossRef]
- Altamirano, C.A.A.; Yokoyama, L.; de Medeiros, J.L.; Araújo, O.D.Q.F. Ethylic or methylic route to soybean biodiesel? Tracking environmental answers through life cycle assessment. *Appl. Energy* **2016**, *184*, 1246–1263. [CrossRef]
- Mandari, V.; Devarai, S. Biodiesel production using homogeneous, heterogeneous, and enzyme catalysts via transesterification and esterification reactions: A critical review. *BioEnergy Res.* **2022**, *15*, 935–961. [CrossRef]
- Likozar, B.; Levec, J. Effect of process conditions on equilibrium, reaction kinetics and mass transfer for triglyceride transesterification to biodiesel: Experimental and modeling based on fatty acid composition. *Fuel Process. Technol.* **2014**, *122*, 30–41. [CrossRef]
- Choedkiatsakul, I.; Ngaosuwan, K.; Cravotto, G.; Assabumrungrat, S. Biodiesel production from palm oil using combined mechanical stirred and ultrasonic reactor. *Ultrason. Sonochem.* **2014**, *21*, 1585–1591. [CrossRef]
- Gholami, A.; Pourfayaz, F.; Maleki, A. Techno-economic assessment of biodiesel production from canola oil through ultrasonic cavitation. *Energy Rep.* **2021**, *7*, 266–277. [CrossRef]
- Tabatabaei, M.; Aghbashlo, M.; Dehghani, M.; Panahi, H.K.S.; Mollahosseini, A.; Hosseini, M.; Soufiyan, M.M. Reactor technologies for biodiesel production and processing: A review. *Prog. Energy Combust. Sci.* **2019**, *74*, 239–303. [CrossRef]
- Naeem, M.; Al-Sakkari, E.; Boffito, D.; Rene, E.; Gadalla, M.; Ashour, F. Single-stage waste oil conversion into biodiesel via sonication over bio-based bifunctional catalyst: Optimization, preliminary techno-economic and environmental analysis. *Fuel* **2023**, *341*, 127587. [CrossRef]
- Zheng, H.; Zheng, Y.; Zhu, J. Recent developments in hydrodynamic cavitation reactors: Cavitation mechanism, reactor design, and applications. *Engineering* **2022**, *19*, 180–198. [CrossRef]
- Farvardin, M.; Samani, B.H.; Rostami, S.; Abbaszadeh-Mayvan, A.; Najafi, G.; Fayyazi, E. Enhancement of biodiesel production from waste cooking oil: Ultrasonic-hydrodynamic combined cavitation system. *Energy Sources Part A Recover. Util. Environ. Eff.* **2019**, *44*, 5065–5079. [CrossRef]
- Maddikeri, G.L.; Gogate, P.R.; Pandit, A.B. Intensified synthesis of biodiesel using hydrodynamic cavitation reactors based on the interesterification of waste cooking oil. *Fuel* **2014**, *137*, 285–292. [CrossRef]

19. Chuah, L.F.; Yusup, S.; Aziz, A.R.A.; Bokhari, A.; Klemeš, J.J.; Abdullah, M.Z. Intensification of biodiesel synthesis from waste cooking oil (Palm Olein) in a Hydrodynamic Cavitation Reactor: Effect of operating parameters on methyl ester conversion. *Chem. Eng. Process. Process. Intensif.* **2015**, *95*, 235–240. [[CrossRef](#)]
20. Laosuttiwong, T.; Ngaosuwan, K.; Kiatkittipong, W.; Wongsawaeng, D.; Kim-Lohsoontorn, P.; Assabumrungrat, S. Performance comparison of different cavitation reactors for biodiesel production via transesterification of palm oil. *J. Clean. Prod.* **2018**, *205*, 1094–1101. [[CrossRef](#)]
21. Gholami, A.; Pourfayaz, F.; Saifoddin, A. Techno-economic assessment and sensitivity analysis of biodiesel production intensified through hydrodynamic cavitation. *Energy Sci. Eng.* **2021**, *9*, 1997–2018. [[CrossRef](#)]
22. Mahmud, R.; Moni, S.M.; High, K.; Carbajales-Dale, M. Integration of techno-economic analysis and life cycle assessment for sustainable process design—A review. *J. Clean. Prod.* **2021**, *317*, 128247. [[CrossRef](#)]
23. Thoppil, Y.; Zein, S.H. Techno-economic analysis and feasibility of industrial-scale biodiesel production from spent coffee grounds. *J. Clean. Prod.* **2021**, *307*, 127113. [[CrossRef](#)]
24. Lee, J.-C.; Lee, B.; Heo, J.; Kim, H.-W.; Lim, H. Techno-economic assessment of conventional and direct-transesterification processes for microalgal biomass to biodiesel conversion. *Bioresour. Technol.* **2019**, *294*, 122173. [[CrossRef](#)]
25. Gordon, R.; Gorodnitsky, I.; Grichko, V. Process for Producing Biodiesel through Lower Molecular Weight Alcohol-Targeted Cavitation. U.S. Patent 8,981,135, 17 March 2015.
26. Ihoeghian, N.A.; Usman, M.A. Exergetic evaluation of biodiesel production from rice bran oil using heterogeneous catalyst. *J. King Saud Univ. Eng. Sci.* **2018**, *32*, 101–107. [[CrossRef](#)]
27. Al-Saadi, L.S.; Eze, V.C.; Harvey, A.P. Techno-economic analysis of processes for biodiesel production with integrated co-production of higher added value products from glycerol. *Biofuels* **2020**, *13*, 489–496. [[CrossRef](#)]
28. Santori, G.; Di Nicola, G.; Moglie, M.; Polonara, F. A review analyzing the industrial biodiesel production practice starting from vegetable oil refining. *Appl. Energy* **2012**, *92*, 109–132. [[CrossRef](#)]
29. Chuah, L.F.; Klemeš, J.J.; Yusup, S.; Bokhari, A.; Akbar, M.M.; Chong, Z.K. Kinetic studies on waste cooking oil into biodiesel via hydrodynamic cavitation. *J. Clean. Prod.* **2017**, *146*, 47–56. [[CrossRef](#)]
30. Trejo-Zárraga, F.; de Jesús Hernández-Loyo, F.; Chavarria-Hernández, J.C.; Sotelo-Boyás, R. Kinetics of Transesterification Processes for Biodiesel Production. In *Biofuels—State of Development*; IntechOpen: London, UK, 2018; pp. 149–179.
31. Brennen, C.E. *Cavitation and Bubble Dynamics*; Oxford University Press: Oxford, UK, 1995.
32. Omelyanyuk, M.; Ukolov, A.; Pakhlyan, I.; Bukharin, N.; El Hassan, M. Experimental and Numerical Study of Cavitation Number Limitations for Hydrodynamic Cavitation Inception Prediction. *Fluids* **2022**, *7*, 198. [[CrossRef](#)]
33. Winterbone, D.E.; Turan, A. Chapter 15—Combustion and Flames. In *Advanced Thermodynamics for Engineers*, 2nd ed.; Elsevier: Amsterdam, The Netherlands, 2015. [[CrossRef](#)]
34. Aigba, P.A.; Emovon, I.; Samuel, O.D.; Enweremadu, C.C.; Abdeljawad, T.; Al-Mdallal, Q.M.; Afzal, A. Exergetic Assessment of Waste Gas to Energy in a Novel Integrated NGL Recovery and Power Generation Plant. *Front. Energy Res.* **2022**, *9*, 798896. [[CrossRef](#)]
35. Szargut, J. Chemical exergies of the elements. *Appl. Energy* **1989**, *32*, 269–286. [[CrossRef](#)]
36. Szargut, J.; Styrylska, T. Approximate Evaluation of the Exergy of Fuels. *Brennst. Waerme Kraft* **1964**, *16*, 589–596.
37. Tsatsaronis, G.; Lazzaretto, A. SPECO: A systematic and general methodology for calculating efficiencies and costs in thermal systems. *Energy* **2006**, *31*, 1257–1289.
38. Boyano, A.; Blanco-Marigorta, A.; Morosuk, T.; Tsatsaronis, G. Exergoenvironmental analysis of a steam methane reforming process for hydrogen production. *Energy* **2011**, *36*, 2202–2214. [[CrossRef](#)]
39. Li, Q.; Lin, Y. Exergy analysis of the LFC process. *Energy Convers. Manag.* **2016**, *108*, 348–354. [[CrossRef](#)]
40. Michalakakis, C.; Fouillou, J.; Lupton, R.C.; Gonzalez Hernandez, A.; Cullen, J.M. Calculating the chemical exergy of materials. *J. Ind. Ecol.* **2021**, *25*, 274–287. [[CrossRef](#)]
41. Mustapha, S.I.; Bux, F.; Isa, Y.M. Techno-economic analysis of biodiesel production over lipid extracted algae derived catalyst. *Biofuels* **2021**, *13*, 663–674. [[CrossRef](#)]
42. Sinnott, R.; Towler, G. *Chemical Engineering Design: Principles, Practice and Economics of Plant and Process Design*; Butterworth-Heinemann: Boston, MA, USA, 2019.
43. Tsagkari, M.; Couturier, J.; Kokossis, A.; Dubois, J. Early-Stage Capital Cost Estimation of Biorefinery Processes: A Comparative Study of Heuristic Techniques. *ChemSusChem* **2016**, *9*, 2284–2297. [[CrossRef](#)]
44. Mata, T.M.; Pinto, F.; Caetano, N.; Martins, A.A. Economic and environmental analysis of animal fats acidity reduction by enzymatic esterification. *J. Clean. Prod.* **2018**, *184*, 481–489. [[CrossRef](#)]
45. Houghton, J.T.; Meira Filho, L.G.; Lim, B.; Treanton, K.; Mamaty, I.; Bonduki, Y. *Revised 1996 IPCC Guidelines for National Greenhouse Gas Inventories: Workbook*; IPCC: Geneva, Switzerland, 1996.
46. Chuah, L.F.; Yusup, S.; Aziz, A.R.A.; Bokhari, A.; Abdullah, M.Z. Cleaner production of methyl ester using waste cooking oil derived from palm olein using a hydrodynamic cavitation reactor. *J. Clean. Prod.* **2016**, *112*, 4505–4514. [[CrossRef](#)]
47. Ahmad, J.; Yusup, S.; Bokhari, A.; Kamil, R.N.M. Study of fuel properties of rubber seed oil based biodiesel. *Energy Convers. Manag.* **2014**, *78*, 266–275. [[CrossRef](#)]
48. Blanco-Marigorta, A.; Suárez-Medina, J.; Vera-Castellano, A. Exergetic analysis of a biodiesel production process from *Jatropha curcas*. *Appl. Energy* **2013**, *101*, 218–225. [[CrossRef](#)]

49. Velásquez, H.; De Oliveira, S.; Benjumea, P.; Pellegrini, L. Exergo-environmental evaluation of liquid biofuel production processes. *Energy* **2013**, *54*, 97–103. [[CrossRef](#)]
50. Innocenzi, V.; Prisciandaro, M. Technical feasibility of biodiesel production from virgin oil and waste cooking oil: Comparison between traditional and innovative process based on hydrodynamic cavitation. *Waste Manag.* **2021**, *122*, 15–25. [[CrossRef](#)]
51. Mahler, D.G.; Dominikus, B. Responsible use of natural resources: Essential for sustainable growth. In *Atlas of Sustainable Development Goals 2023*; World Bank: Washington, DC, USA, 2023.
52. Sachs, D. From millennium development goals to sustainable development goals. *Lancet* **2012**, *379*, 2206–2211. [[CrossRef](#)]
53. Usaku, C.; Yahya, A.B.; Daisuk, P.; Shotipruk, A. Enzymatic esterification/transesterification of rice bran acid oil for subsequent  $\gamma$ -oryzanol recovery. *Biofuel Res. J.* **2023**, *10*, 1830–1843. [[CrossRef](#)]
54. Al-Saadi, L.S.; Eze, V.C.; Harvey, A.P. A techno-economic analysis based upon a parametric study of alkali-catalysed biodiesel production from feedstocks with high free fatty acid and water contents. *Biofuels* **2022**, *13*, 401–413. [[CrossRef](#)]
55. Oke, E.O.; Okolo, B.I.; Adeyi, O.; Adeyi, J.A.; Ude, C.J.; Osoh, K.; Otolorin, J.; Nzeribe, I.; Darlinton, N.; Oladunni, S. Process Design, Techno-Economic Modelling, and Uncertainty Analysis of Biodiesel Production from Palm Kernel Oil. *BioEnergy Res.* **2021**, *15*, 1355–1369. [[CrossRef](#)]
56. Gengiah, K.; Gurunathan, B.; Rajendran, N.; Han, J. Process evaluation and techno-economic analysis of biodiesel production from marine macroalgae *Codium tomentosum*. *Bioresour. Technol.* **2022**, *351*, 126969. [[CrossRef](#)]
57. Niño-Villalobos, A.; Puello-Yarce, J.; González-Delgado, Á.D.; Ojeda, K.A.; Sánchez-Tuirán, E. Biodiesel and hydrogen production in a combined palm and jatropha biomass biorefinery: Simulation, techno-economic, and environmental evaluation. *ACS Omega* **2020**, *5*, 7074–7084. [[CrossRef](#)]
58. Naveenkumar, R.; Baskar, G. Optimization and techno-economic analysis of biodiesel production from *Calophyllum inophyllum* oil using heterogeneous nanocatalyst. *Bioresour. Technol.* **2020**, *315*, 123852. [[CrossRef](#)]
59. Sakdasri, W.; Sawangkeaw, R.; Ngamprasertsith, S. Techno-economic analysis of biodiesel production from palm oil with supercritical methanol at a low molar ratio. *Energy* **2018**, *152*, 144–153. [[CrossRef](#)]
60. Yusuf, N.; Kamarudin, S. Techno-economic analysis of biodiesel production from *Jatropha curcas* via a supercritical methanol process. *Energy Convers. Manag.* **2013**, *75*, 710–717. [[CrossRef](#)]
61. Zhang, Y.; Dube, M.; McLean, D.; Kates, M. Biodiesel production from waste cooking oil: 1. Process design and technological assessment. *Bioresour. Technol.* **2003**, *89*, 1–16. [[CrossRef](#)]
62. Lee, S.; Posarac, D.; Ellis, N. Process simulation and economic analysis of biodiesel production processes using fresh and waste vegetable oil and supercritical methanol. *Chem. Eng. Res. Des.* **2011**, *89*, 2626–2642. [[CrossRef](#)]

**Disclaimer/Publisher's Note:** The statements, opinions and data contained in all publications are solely those of the individual author(s) and contributor(s) and not of MDPI and/or the editor(s). MDPI and/or the editor(s) disclaim responsibility for any injury to people or property resulting from any ideas, methods, instructions or products referred to in the content.